Ecotoxicology and Environmental Safety 209 (2021) 111776

Contents lists available at ScienceDirect

Ecotoxicology and Environmental Safety

journal homepage: www.elsevier.com/locate/ecoenv

Graphene oxide-silver nanoparticle hybrid material: an integrated nanosafety study in zebrafish embryos

Aline M.Z. de Medeiros [a,b,c], Latif U. Khan [a], Gabriela H. da Silva [a], Carlos A. Ospina [a], Oswaldo L. Alves [d], Vera Lúcia de Castro [c], Diego Stéfani T. Martinez [a,b,d,*]

[a] Brazilian Nanotechnology National Laboratoy (LNNano), Brazilian Center for Research in Energy and Materials (CNPEM), Campinas, São Paulo State, Brazil
[b] Center of Nuclear Energy in Agriculture (CENA), University of São Paulo (USP), Piracicaba, São Paulo State, Brazil
[c] Brazilian Agricultural Research Corporation (Embrapa Environment), Jaguariúna, São Paulo State, Brazil
[d] Laboratory of Solid State Chemistry (LQES) and NanoBioss Laboratory, University of Campinas (Unicamp), Campinas, São Paulo State, Brazil

ARTICLE INFO

Edited by: Professor Bing Yan

Keywords:
Nanohybrids
Chorion
Nanoecotoxicology
Nanotoxicity
Alternative methods

ABSTRACT

This work reports an integrated nanosafety study including the synthesis and characterization of the graphene oxide-silver nanoparticle hybrid material (GO-AgNPs) and its nano-ecotoxicity evaluation in the zebrafish embryo model. The influences of natural organic matter (NOM) and a chorion embryo membrane were considered in this study, looking towards more environmentally realistic scenarios and standardized nanotoxicity testing. The nanohybrid was successfully synthesized using the $NaBH_4$ aqueous method, and AgNPs (~ 5.8 nm) were evenly distributed over the GO surface. GO-AgNPs showed a dose-response acute toxicity: the LC_{50} was 1.5 mg L^{-1} for chorionated embryos. The removal of chorion, however, increased this toxic effect by 50%. Furthermore, the presence of NOM mitigated mortality, and LC_{50} for GO-AgNPs changed respectively from 2.3 to 1.2 mg L^{-1} for chorionated and de-chorionated embryos. Raman spectroscopy confirmed the ingestion of GO by embryos; but without displaying acute toxicity up to 100 mg L^{-1}, indicating that the silver drove toxicity down. Additionally, it was observed that silver nanoparticle dissolution has a minimal effect on these observed toxicity results. Finally, understanding the influence of chorion membranes and NOM is a critical step towards the standardization of testing for zebrafish embryo toxicity in safety assessments and regulatory issues.

1. Introduction

Graphene oxide (GO) is a two-dimensional carbon nanomaterial. It is composed of carbon atoms organized in a hexagonal lattice, forming one flat sheet, containing oxygenated groups. Due to its extraordinary properties (e.g., thermal resistance, electrical conductivity, optical transparency, mechanical strength and chemical versatility), GO has been explored for many applications in materials science, nanomedicine, biotechnology and environmental technology (Ren and Cheng, 2014; Dideikin and Vul, 2019). GO-metal hybrid materials make up an emerging class of advanced materials based on graphene oxide. The goal of synthetizing new GO-based nanohybrid materials, coupling different metallic nanoparticles, is to enhance material functionality and/or to obtain multifunctional properties, working towards superior performance and new applications (Yin et al., 2015; Fonseca et al., 2018; Hassandoost et al., 2019).

Silver nanoparticles (AgNPs) are collectively one of the most extensively used types of nanomaterial, this being due to their antibacterial capability, catalytic activity, and optical and photo-thermal properties (McGillicuddy et al., 2017).

To this end, the GO-AgNPs hybrid material possesses a substantial potential for innovation; demonstrating promising applications in different sectors, such as environmental engineering (Koushik et al., 2016), electrochemical sensing and catalysis (Sharma et al., 2017; Xu et al., 2017), agriculture (Chen et al., 2016) and biomedicine (De Moraes, 2015; Zhou et al., 2016). Interestingly, GO-AgNPs may possess a use as a membrane material for seawater desalination and remediation, due to their hydrophobicity and antimicrobial properties (Soroush et al., 2015). This nanohybrid might also be applied in a wide variety of electrochemical sensors and biosensors for the detection of tryptophan (Li et al., 2013), ammonia (Kavinkumar and Manivannan, 2016), glucose (Hoa et al., 2017) and 4-nitrophenol (Ahmad et al., 2020). In

* Corresponding author at: Brazilian Nanotechnology National Laboratoy (LNNano), Brazilian Center for Research in Energy and Materials (CNPEM), Campinas, São Paulo State,Brazil.
E-mail address: diego.martinez@lnnano.cnpem.br (D.S.T. Martinez).

https://doi.org/10.1016/j.ecoenv.2020.111776
Received 10 August 2020; Received in revised form 4 December 2020; Accepted 5 December 2020
Available online 17 December 2020

addition, GO-AgNPs have also been explored for the development of drug-delivery systems (Encarnacion-Rosado et al., 2016) and novel bio-imaging materials (Kundu et al., 2017). Due to their promising applications, it is imperative to support studies that comprise the risk and toxicity evaluation of nanohybrid materials at an early stage of their synthetic production and research development, to minimize undesirable impacts on human and environmental health towards sustainable nanotechnology and responsible innovation (Hutchison, 2016). In fact, the safe-by-design of this nanomaterial needs to include a minimum amount of information on the tested materials (i.e. physical-chemical characterization), the influence of the surrounding environment (i.e. colloidal behaviour and natural organic matter) and the biological model organism, for a toxicity assessment (Lin et al., 2018). However, and although many studies have reported on the toxic effects of exposure to the graphene family and metallic nanoparticles (as silver nanoparticles) in various biological models, the nano-ecotoxicology and environmental safety aspects of GO-based nanohybrids are poorly understood (De Luna et al., 2016; Kim et al., 2018). Special attention to the environmental risks of nanohybrids is therefore required (Saleh et al., 2014, 2015; Plazas-Tuttle et al., 2015).

Nanomaterials can be transported in aquatic ecosystems, which makes them available for uptake by aquatic organisms (Park et al., 2017). The predicted environmental concentrations (PECs) for carbon-based nanomaterial and AgNPs in an aquatic compartment lie in the 0.02–6.0 ηg.L^{-1} range (Mottier et al., 2017; Zhao et al., 2020). Furthermore, natural organic matter (NOM) is one crucial factor that influences the aggregation state of nanomaterial in aquatic systems (Grillo et al., 2015; Markiewicz et al., 2018) therefore it should be considered in the nano-ecotoxicological evaluation towards more environmentally realistic scenarios (Lowry et al., 2014). Nanomaterial-NOM interactions are a fundamental issue in the understanding of nanomaterial mobility and consequently bioavailability for different organisms (Su et al., 2017; Castro et al., 2018). The presence of NOM may modify the dissolution rate of metallic nanoparticles, including AgNPs (Zhang et al., 2018). Thus, NOM interaction with the AgNP surface might improve the colloidal stability and decrease the Ag^{+} release, which would have a direct influence on the toxicological profile of AgNPs (Gunsolus et al., 2015). It is therefore important to study the effects of NOM during the ecotoxicity assessment of GO-AgNP nanohybrids.

The Zebrafish (*Danio rerio*) is a promising model for environmental and human health studies because it presents an exceptional set of characteristics (Chakraborty et al., 2016; Lee et al., 2017; Haque and Ward, 2018). A recent critical challenge for nanotoxicity assessments using zebrafish embryos is the presence of a chorion membrane (Sieber et al., 2019). This biological structure presents pore channels of 0.5–0.7 mm in diameter, which partly isolate the larvae from the environment until hatching (Lin et al., 2013). The membrane penetration ability is strongly correlated with nanoparticle size, and in most cases, this characteristic may block the entrance of nanomaterial (Chen et al., 2020). For example, should GO adhere to this membrane, a gas exchange will be prevented from occurring. This hypoxic microenvironment can then induce hatching delay and malformation (Su et al., 2017). The removal of this membrane commences the direct exposition of the embryo to nanomaterial and simultaneously guarantees that the effects are provoked by nanoparticles, and not by the hypoxic environment – which potentially causes secondary morphological deformations (Panzica-Kelly et al., 2015; Khan et al., 2019).

Other parameters such as lipophilicity, charges, and specific molecular conformations, may also play an important role in the definition of the uptake of chemicals across the chorion of zebrafish embryos (Pelka et al., 2017). The removal of the chorion protection enables us to begin exposition of the embryo at an early life stage when the fish has begun its organogenesis (Chen et al., 2015), and consequently to change its toxicological profile. For example, TiO_2 and graphitic carbon nitride (g-C_3N_4) nanomaterial showed no acute toxicity to zebrafish embryos with chorion protection. Nevertheless, de-chorionated embryos exhibited an increase in mortality due to direct nano-bio interaction between the nanomaterial and the embryonic epidermis (He et al., 2020). It is therefore fundamental to understand the influence of chorion on the toxicity of nanohybrids in order to support the development of standardized nanotoxicity testing.

The synthetic method used to produce GO-AgNPs critically influences their final material properties. The reducing agent used in the reaction (Çiplak et al., 2015), different ratios of GO and Ag^{+} (Çiplak et al., 2015; Kavinkumar and Manivannan, 2016) or surface microchemicals (quantity of oxygen function groups or debris) present in raw GO (Faria et al., 2012) could provide distinct nanohybrid material. Therefore, it is necessary to use an integrated approach (chemical and physical techniques) to better understand the different aspects related to chemical composition (e.g., functional surface groups, oxidation states, silver loading) and structure (e.g., metal particle size and shape, crystalline phase, chemical bonds); especially, when considering nano-toxicological studies (Fadeel et al., 2018).

In this work, we performed an integrated nanosafety study for an ecotoxicity assessment of the emerging GO-AgNPs nanohybrid using zebrafish embryos as a biological model. The following aspects were studied: i) GO-AgNPs nanohybrid synthesis and characterization; ii) nanohybrid dispersion stability and silver dissolution in the zebrafish medium; and iii) toxicity assessment on the zebrafish embryos. The influences of chorion membrane removal and NOM on the toxicity of GO-AgNPs were reported towards more realistic and standardized methods for nano-ecotoxicology research and regulatory issues.

2. Material and methods

2.1. Synthesis of nanomaterials

2.1.1. Graphene oxide

GO sheets were synthesized from graphite flakes (purchased from Sigma-Aldrich, Lot#MKBW0432V) by the modified Hummers method (Becerril et al., 2008). Briefly, a graphite flake (5.0 g) and $NaNO_3$ (3.75 mg) were placed in a round-bottomed flask and H_2SO_4 (370 mL; A.R.) was added in an ice bath under continuous stirring for 20 min. Then $KMnO_4$ (22.5 g) was slowly added over about one hour. The mixture reaction was stirred for 72 h at room temperature, which was then diluted with ultrapure water (300 mL). The mixture was stirred again for one more hour at 95 °C. After the temperature fell to 60 °C, H_2O_2 (15 mL; 30%) was added to reduce the $KMnO_4$ residual and the liquid was left to stand overnight. The resultant mixture was brilliant yellow.

The mixture was centrifuged (6000 rpm; 15 min) and rinsed with 1.0 L of an aqueous H_2SO_4 solution (3%) and H_2O_2 (0.5%) to remove oxidant ions and inorganic impurities. The resulting product was dialyzed (cut-off: 14,000 kDa) against deionized water for 3 days. The graphene oxide dispersion was lyophilized to produce GO powder, which was stored in a sealed vessel at room temperature. Stock-suspensions of 1 mg mL^{-1} were prepared in ultrapure water by sonication in an ultrasonic bath (CPXH; Cole-Parmer) at 40 Hz for 80 min

2.1.2. Graphene oxide-silver nanoparticle hybrid material

A GO-AgNPs nanohybrid was obtained using $NaBH_4$ as a reducing agent for the $AgNO_3$ (Mahmoudi et al., 2015). Previously prepared GO (20 mg) was dispersed in ultrapure water (40 mL) using an ultrasonic bath (1 h). This suspension was mixed with $AgNO_3$ (purchased from Sigma Aldrich, purity >99.0% per 0.004 mol L^{-1}; 20 mL) in an ice bath under continuous stirring for 1 h. Then $NaBH_4$ (63 mg) was slowly added and the reaction was kept under stirring overnight to ensure that the silver was reduced entirely. The GO-AgNP stock dispersion was stored in a sealed vessel protected from light.

2.2. Characterization of nanomaterials

The absorbance of GO and GO-AgNP dispersions was recorded using UV–vis spectroscopy (micro plate spectrophotometer; MultiskanTM; Thermo Scientific). The appearance of a Plasmon resonance band at 390–410 nm was used to confirm the formation of AgNPs. The high-resolution X-ray diffraction (XRD) patterns (XDR6000, Shimadzu) of dry samples were measured using Cu Kα1 radiation (λ: 1.5406 Å) at 40 kV in the range of $2\theta = 5–90^{\circ}$. The shape, surface morphology and thickness of the graphene sheets were evaluated through topography images from atomic force microscopy (AFM). This analysis was conducted in ambient conditions using a Multimode 8 microscope with a Nano Scope 5 controller, with Peakforce tapping (Bruker). Images were treated on Gwyddion software. We obtained size distributions of GO sheets by measuring ~130 flakes on ImageJ software.

Transmission Electron Microscopy (TEM) analyses were carried out using a JEM-2100 microscope, operating in TEM mode at 200 kV and a Double Aberration Corrected Titan Cubed Themis, performing at 80 and 300 kV. TEM samples were prepared by dropping 3 mL of diluted dispersion on Cu grids with a Lacey carbon film. The size distributions of AgNPs on GO sheets we obtained by measuring 100 nanoparticles, using ImageJ software.

Raman spectra were measured using XploRA™ PLUS Confocal Raman Microscope (Horiba Jobin Yvon). The excitation wavelength was 638 nm. The scanned spectral range was 400–4000 cm^{-1} with a spectral resolution of >1.4 cm^{-1} and accumulation times were typically five collections of 5 s. The samples were prepared by spreading a small quantity of solid powder on glass microscope slides and Raman spectra were collected at random points under a magnification of 100X the objective.

X-ray photoelectron spectroscopic (XPS) analysis was performed to verify the surface chemistry of GO and its nanohybrid material. This analysis was carried out at K-Alpha XPS (Thermo Fisher Scientific). Survey spectra were measured (i.e., full-range) to identify the elemental composition of materials. High-resolution spectra of carbon and silver (only to nanohybrid) were acquired to determine the functional groups and silver state. The data were analysed using Thermo Advantage software (version 5.957).

Thermo gravimetric analysis (TGA) was performed using a thermogravimetric analyzer (STA 449 F3Jupiter@; NETZSCH; 10 °C min^{-1}; synthetic air flow rate of 50 mL min^{-1}).

2.3. Dispersion stability monitoring

The dispersion stability of nanomaterials (100 mg L^{-1}) in the absence and presence of NOM (Suwannee River NOM; International Humic Substances Society; fixed concentration: 20 mg L^{-1}) was pursued by spectrophotometric analyses (micro plate spectrophotometer; Multiskan GO; Thermo Scientific). The absorbance of samples at 230 nm was used to compare stabilities. Surface charges (zeta potentials) of the material were measured by electrophoretic light scattering (ELS) at Zetasizer Nano ZS (Model ZEN3600, Malvern). The dispersion was prepared in ultrapure water (as a reference control) and the zebrafish embryo medium (used in a biological assay). The samples were maintained static for 72 h, and 100-μL aliquot was removed every 24 h from the surface of the dispersion. Each measurement was carried out with three independent measures. We used the OECD 318 guideline (OECD, 2017), with modifications, when monitoring the colloidal dispersion stability of nanomaterial in ultrapure water and the zebrafish medium.

The NOM concentration used in the present study presented itself in the US EPA test guidelines (US EPA, 1996) due to being representative of surface and groundwater environmental conditions (Janknecht et al., 2009; Wang et al., 2015; Clemente et al., 2017).

2.4. Zebrafish embryo toxicity testing

In vivo assays are based on the fish embryo acute toxicity (FET) test (OECD. 236, 2013) (OECD, 2013) modified for chorion removal. Briefly, zebrafish eggs were collected one hour after a natural mating of wild-type adults and washed with reconstituted water. The eggs were selected under microscopy for their viability to assay. The egg was considered non-viable if the embryo was delayed, not correctly developed, or dead (a coagulated egg). 24 h post-fertilization (hpf), the eggs were de-chorionated mechanically with forceps (Dumont™ no.5) according to the reported procedure (Henn and Braunbeck, 2011).

The exposition commenced at 24 hpf and was performed for 72 h (24–96 hpf) without any renovation in the medium. The two groups of embryos were exposed to the same range of concentrations, as follows. Salts/nanomaterial (5 different expositions): the control (medium only); $AgNO_3$; GO; GO-AgNPs; and a filtrate-only control. Moreover, the co-exposure with NOM (Suwannee River NOM, International Humic Substances Society, fixed concentration at 20 mg L^{-1}) was also evaluated and all experiments were carried out in triplicate. Thus, the breakdown for the number of treatments was as follows: two groups of embryos (with and without chorion) in five different substances or nanomaterial types, multiplied by two (presence or absence of NOM), giving us 20 treatments in total.

The filtrate-only control was also performed to assess either impairment caused by dissolved ions throughout the assay. The dispersion then of GO-AgNPs in the zebrafish medium (100 mg L^{-1}) was kept under the same conditions (test media, photoperiod, temperature) and time (72 h) of the assay; after this, the dispersion was filtrated (Millipore; 0,1 nm; PTFE). The remaining filtrate was diluted and used in a FET assay (Petersen, 2015). The dilution factor was similar to making 0.5; 1; 2 and 4 mg L^{-1}; that is, 200; 100; 50 and 25 times. The test was performed under the same conditions as the OECD standard test, as described below. For every group, 10 embryos (3 replicates) were exposed to 20 mL of dispersion (2 mL/egg) and incubated in Petri dishes at 28 °C and a 14 h:10 h, light: dark cycle until after 96 hpf, live larvae are photographed with a stereomicroscope (Stereo Discovery V20, Zeiss). The fish embryo was kept in reconstituted water (fish embryo medium), prepared as moderately hard water (USEPA, 2002). Briefly, into distilled water was added $NaHCO_3$ (96 mg L^{-1}), $MgSO_4$ (60 mg L^{-1}), KCl (4 mg L^{-1}), $CaSO_4$ (60 mg L^{-1}), and pH 7.5 ± 0.5. The parameters assessed in FET were: i) mortality, ii) malformation, iii) edema, iv) hatching, v) total length and vi) yolk sac size. The lethal concentration (LC_{50}) value (i.e. a concentration that kills 50% of the embryos during the observation period) was calculated based on the mortality rate and was used when comparing the two groups.

The Embrapa Environment's Ethics Commission approved the animal handling procedures for Animal Use (CEUA-Embrapa Environment, protocol number 004/2017).

2.5. Chemical transformation of the GO-AgNPs nanohybrid in the zebrafish medium

Chemical changes due to exposure to the environment (i.e. light, temperature, test media, presence of NOM) were assessed in the GO-AgNPs during the toxicity assay. For this, a dispersion (100 mg L^{-1}) of GO-AgNPs in the medium test was prepared and maintained in the same conditions as the test. After 72 h, the liquid was centrifuged (14,000 rpm; 1 h) and the supernatant was discarded. The pellet was re-suspended in ultrapure water and the chemistry surface analysed by XPS. The control experiment was performed using the same procedure, but the dispersion (100 mg L^{-1} of GO-AgNPs in medium test) was centrifuged immediately. In addition to this, the contribution of the presence of NOM (20 mg L^{-1}) was also evaluated.

2.6. Data analysis

The lethal concentration (LC_{50}) values (i.e. a concentration that kills 50% of the embryos during the observation period) and 95% confidence intervals were calculated using Probit analysis of dose-mortality data from bioassay studies in PriProbit software. Data were analysed regarding normality distribution and homogeneity of variance (homoscedasticity) using (respectively) Shapiro-Wilk's and Levene's tests. As the results were normal and homoscedastic, differences between means of treatments were evaluated using variance analysis (ANOVA-one way). Differences between embryos with and without chorion were analysed using ANOVA-two way. The tests were followed by Dunnet's multiple comparisons test with a confidence interval of $p < 0.05$. Statistical analyses and graphs were generated on Origin software (version 8.5). All data are presented as the means ± SD.

3. Results and discussion

The GO-AgNPs nanohybrid demonstrated the ability to be synthetized through in situ methods, in which the growth of the metal nanoparticle occurs directly on the graphene oxide flake, or through *ex situ* methods, in which a premade nanoparticle is attached to the graphene oxide surface. Different methods may be applied for each approach. The in situ approach, for example, includes reduction by chemical agents, and hydrothermal and electrochemical techniques (Yin et al., 2015). In this study, the one-step aqueous methods using the reduction method to form a GO-AgNPs nanohybrid were chosen. In general, this technique uses a metal precursor (e.g. $AgNO_3$) mixture with GO dispersion, and a chemical agent simultaneously reduces it. The defects and oxygen-functional groups provide the attachment of free Ag^+ onto a GO surface through electrostatic interactions, and the addition of reducing agents, enabling the synthesis of AgNPs (Faria et al., 2012). The synthesis of nanohybrid in this study used $NaBH_4$ as a reduction agent and the growth of AgNPs was controlled by the low temperature (ice bath).

Several substances may be used to reduced Ag^+ in the presence of GO for synthesis of the nanohybrid, such as sodium citrate (Faria et al., 2012, Tang et al., 2013), potassium hydroxide (Pasricha et al., 2009), or hydrazine hydrate (Çiplak et al., 2015). Environmentally friendly (green) synthesis has also been developed: *Hibiscus sabdariffa* extract

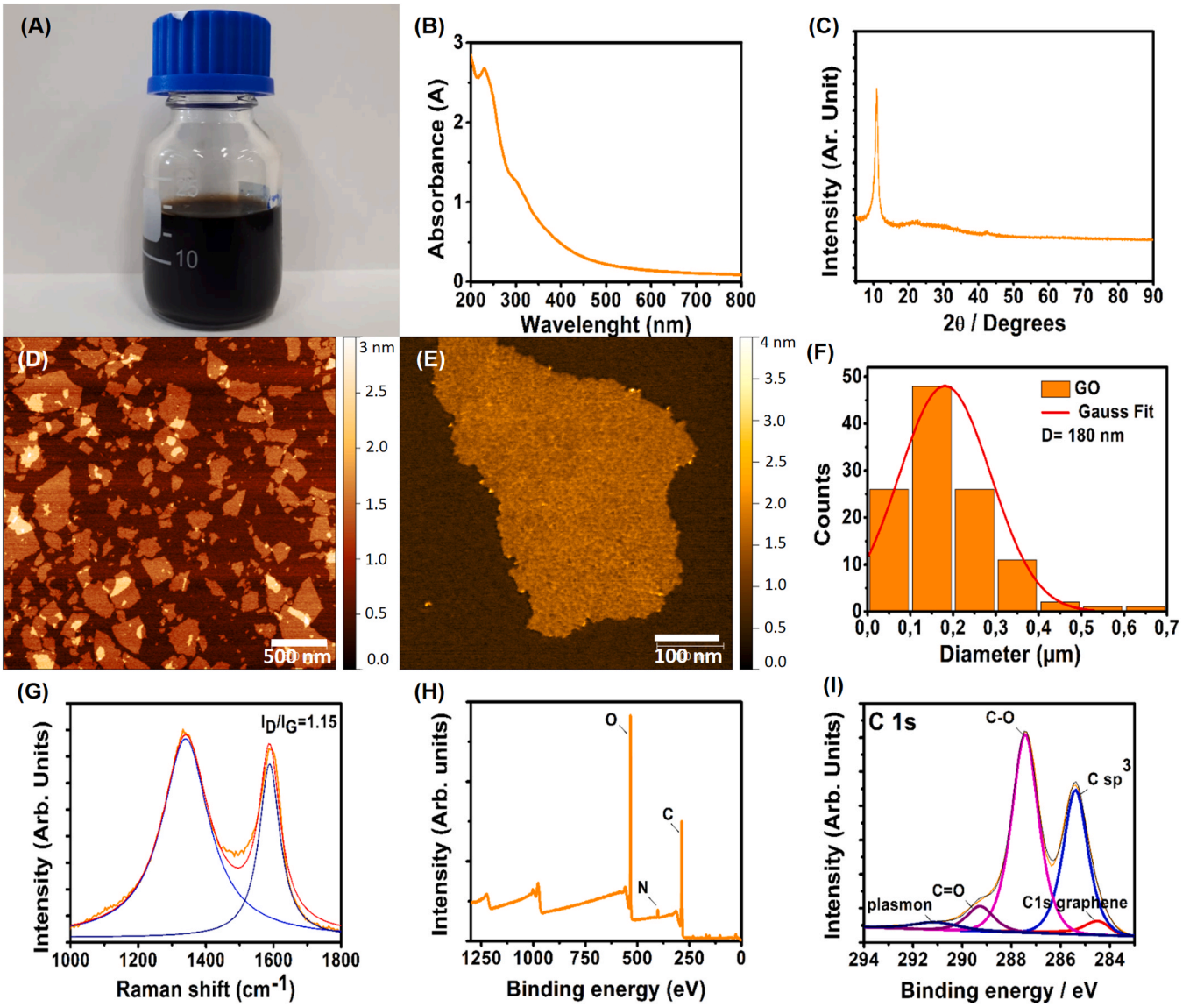

Fig. 1. Graphene oxide (GO) characterization. Stock-dispersion at 1.0 g L^{-1} (A), UV-Vis absorption spectrum (B). XRD pattern (C). AFM topography image (D). AFM topography image zoomed in (E). Histogram of size distribution of GO flakes (F). Raman Spectrum, D and G bands (G). Survey XPS spectrum (H). High-resolution C1s XPS spectrum (I).

(Nazari and Movafeghi, 2018), glucose (Shao et al., 2015; Kim et al., 2018), and ascorbic acid (Kavinkumar and Manivannan, 2016) have each been used to form the GO-AgNPs nanohybrid.

However, the mechanism of silver nanoparticle nucleation and growth on GO surfaces needs to be elucidated in more detail by exploring advanced characterization methods. Furthermore, graphene-metal nanohybrids exhibit emergent properties, which might be able to modify the characteristics of its precursor (Wang et al., 2019). Thus, a complete nanohybrid characterization is crucial to elucidate the interactions of nanomaterial within biological and environmental systems (Fadeel et al., 2018).

3.1. Graphene oxide characterization

The final GO stock-dispersion (1.0 g L^{-1}) shows a light brown colour (Fig. 1-A). The optical characteristics of GO were verified by UV-Vis spectroscopy in the range of 200–800 nm. The absorption spectrum of GO exhibited an absorption band centred at 230 nm, which is characteristic of π-π * electronic transitions of C-C aromatic bonds (De Moraes, 2015) (Fig. 1-B). The XRD pattern (Fig. 1-C) exhibits diffraction peaks at 2θ values of 10.9 and 42.3 that may be indexed as (002) and (100) diffraction plans of hexagonal structure graphene oxide.

AFM images of GO reveals size distribution from 50 to 650 nm, the mean size being 180 nm. A histogram of particle sizes was constructed by counting more than one hundred flakes. Besides this, the topography images showed their average thickness to be around 1 nm, which reveals a single-layer structure of GO sheets. However, this was larger than that for pure graphene (0.335 nm), probably because of oxygenated groups present in GO (Liu et al., 2017) (Fig. 1-D, E, F).

Raman spectroscopy is a useful technique that provides remarkable information on the structural disorder in sp^2 hybridized carbon materials, such as graphene. The Raman scattering spectrum (Fig. 1-G) of GO typically presents two peaks: the D-Band and G-Band. The first band, D, was located at ~1332 cm^{-1} and assigned to the breathing mode of κ-point phonons, with A1g symmetry. This band has thus resulted in a disordered structure of graphene. The prominent D peak originates from the structural imperfections created by introducing hydroxyl and epoxide groups in the carbon structure during the oxidation of graphene flakes. The G band (~1590 cm^{-1}) is attributed to the tangential stretching mode of the E2g phonon in the sp^2 carbon atoms (Dresselhaus et al., 2010). In this way, the ratio between intensities of the D-Band (I_D) and G-Band (I_G) could indicate the proportion of defects in flakes. In GO flakes, the calculated ratio was 1.15, which shows a high presence of defects that confirm the presence of oxygenated groups in graphene flakes.

The chemical composition of the GO surface was determined by X-ray photoelectron spectroscopy (XPS). Survey spectrum (Fig. 1-H) showed the presence of carbon (66.5 ± 0.9%), oxygen (31.4 ± 0.6%) and nitrogen (2.0 ± 0.6%). A high percentage of oxygen confirmed the oxidation of GO. The high-resolution C1s spectrum (Fig. 1-I) reveals the functional groups (C-O and COO) present on the surface of GO. Table 1 shows the respective percent contents of each group derived from the deconvoluted C1s spectrum.

Thermogravimetric analysis was acquired in order to access the thermal stability of GO and the result is presented in the Supplementary Material (Fig. S1). GO displays a two steps decomposition. The first mass loss, that occur in the range of 150 – 200 °C, is attributed to the decomposition of oxygenated groups and the second, at 500 °C is assigned to the decomposition of the graphitic portion.

Table 1
Surface chemistry elemental analysis in high-resolution C1s of GO by X-ray photoelectron spectroscopy.

Chemical groups	Binding energy (eV)	% Atomic
Graphitic / aromatic carbon (-C=C-)	284.1	5.34
Aliphatic carbon (-C-C-)	285.0	31.97
Epoxy/hydroxyl groups (C-O)	286.9	45.52
Carbon / ester (COO)	288.7	9.11
π- π * transition in aromatic	290.7	8.07

3.2. GO-AgNPs nanohybrid characterization

GO-AgNPs stock-dispersion presents a black-green colour (Fig. 2-A). The UV-Vis absorption spectrum (Fig. 2-B) shows an absorption band at 400 nm that refers to the plasmon resonance due to the formation of AgNPs. The XRD pattern of the GO-AgNPs nanohybrid material exhibits a broad diffraction peaks at a 2θ value of 25.0 that corresponds to the (002) graphene diffraction plan. This result suggests that graphene oxide is partially reduced to graphene during nanohybrid material synthesis. In addition, the XRD pattern of GO-AgNPs also presents diffraction reflections at 2θ values of 38, 44.1, 64.3 and 77.4, corresponding to the (111), (200), (220) and (311) diffraction planes of the Ag cubic phase (ICDD/PDF 01–1167), confirming that decoration of the graphene sheet with Ag nanoparticles occurs (Fig. 2 – C).

TEM images of GO-AgNPs show the formation of uniformly distributed AgNPs (black dots) on the surface of the GO sheet. The AgNPs are of a mean size of 5.8 nm (Fig. 2- D, E, F, G). Furthermore, Das et al. (2011); Mahmoudi et al. (2015) prepared GO-AgNPs nanohybrid using borohydride as a reducing agent of silver nitrate in a GO dispersion. The distribution size of AgNPs was very similar (5–10 nm and 2–5 nm, respectively).

Negative surface charges carried by functional groups in the GO flakes allowed electrostatic interaction with the Ag^+ ion and provided a platform for the nucleation and growth of nanoparticles. The Raman spectrum of the GO-AgNPs nanohybrid (Fig. 2-I) displays a considerable increase in the ratio of the intensities of the D and G bands (I_D/I_G) from 1.15 to 1.35, after decorating GO nanoflakes with AgNPs. This increase in the I_D/I_G value may be attributed to a rise in degree of disorder in the graphene matrix due to the interaction of GO with AgNPs. Similarly, Chen et al. (2018) observed an enhancement of the I_D/I_G ratio after AgNPs anchored into GO flakes, due to an increase in the structural defects of graphene. In this case, they found an I_D/I_G value of 1.098 for GO; after hybrid formation, the ratio modified to 1.31.

The XPS survey spectrum (Fig. 2-J) revealed that the surface chemistry of GO-AgNPs is composed of 67.45% carbon, 29.67% oxygen, and 2.88% silver. The high-resolution de-convoluted C1s spectrum (Fig. 2-K) showed the peaks at binding energies of 285, 286.9, and 288.7 eV, attributing to the C–C, C–O and O–C=O bonds, as exhibited respectively in Table 2. The lowering of the epoxy/hydroxyl group content in the hybrid material manifested that sodium borohydride also reduced the epoxy and aldehyde groups present in the GO sheet. Furthermore, the Ag spectrum (Fig. 2-L) shows the characteristic peaks for Ag3d at 368.3 and 374.3 eV corresponding to the $Ag3d_{5/2}$ and $Ag3d_{3/2}$, respectively, suggesting an interaction of AgNPs with graphene oxide sheets. Furthermore, the Ag spectrum (Fig. 2-L) was composed mostly of Ag metal (~99%). The presence of silver mostly in metallic form indicates that the growth of AgNPs in GO sheets has also been observed in previous studies (De Moraes, 2015; Shao et al., 2015; Kellici et al., 2016).

The thermal gravimetric analysis (TGA) shows the two steps decomposition similarity to GO (Supplementary Material; Fig. S1). However, the nanohybrid displays reduction of decomposition temperatures. This behaviour suggest that AgNPs act as catalysts (De Faria et al., 2014; De Moraes, 2015). Moreover, the residuals content, approximately 60%, could be related to the silver mass proportion on GO-AgNPs.

3.3. The influence of NOM on the dispersion stability of GO and GO-AgNPs in ultrapure water and the ZZ Zebrafish medium

The fish embryo medium is a type of standard synthetic water

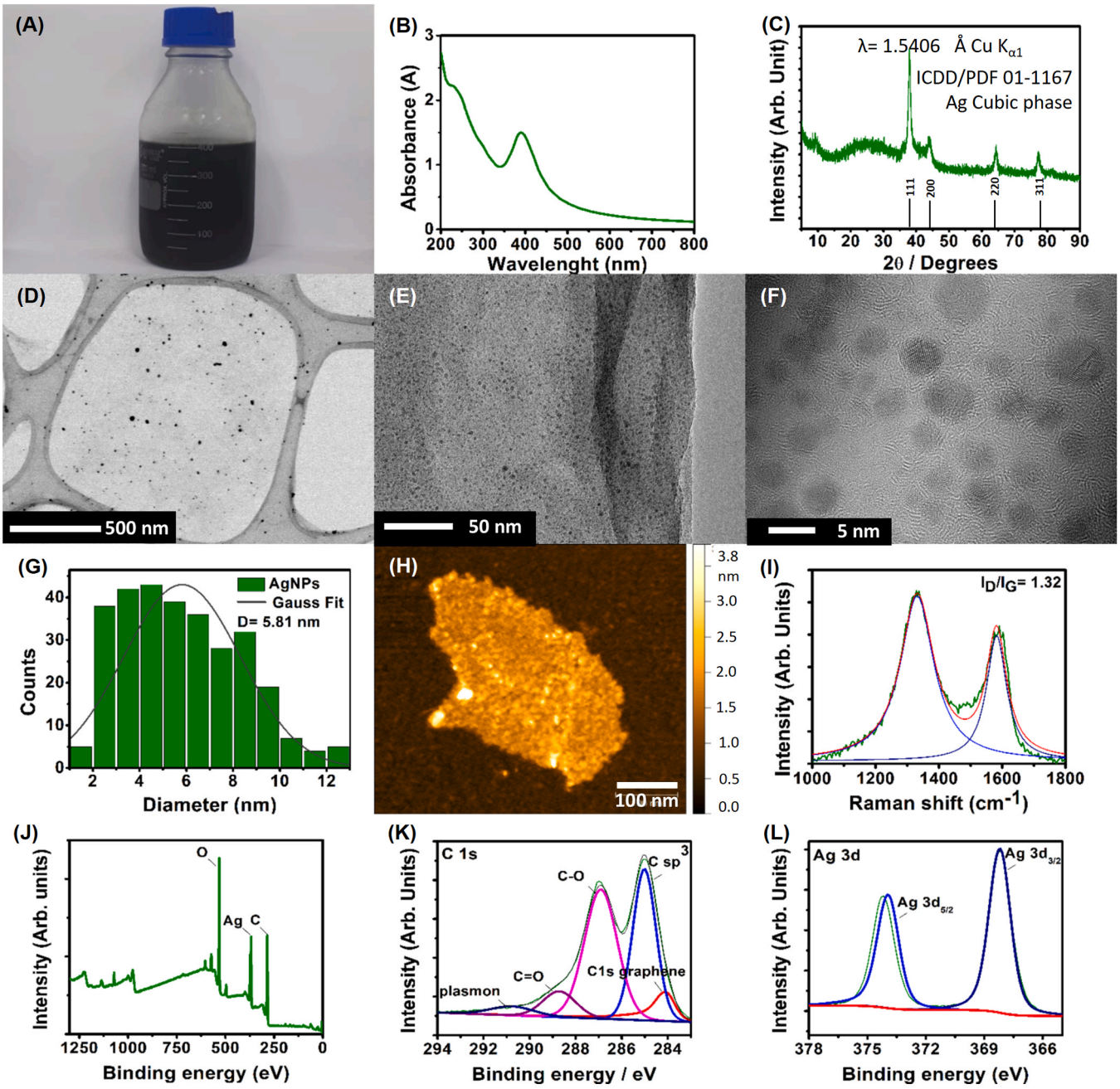

Fig. 2. GO-AgNPs nanohybrid characterization. Stock-dispersion at 0.5 g L^{-1} (A), UV-Vis absorption spectrum with plasmon resonance @ 400 nm (B). XRD pattern (C). Typical TEM images (D). TEM image, high resolution (E). Monochromated HRTEM of AgNPs (F). Histogram AgNPs size distribution decorated on a GO flake (G); AFM topography image (H). Raman Spectrum, D and G bands (I). Survey XPS spectrum (J). High-resolution C1s XPS spectrum (K). High-resolution Ag spectrum (L).

Table 2
Surface chemistry elemental analysis in high-resolution C1s and of GO-AgNPs by X-ray photoelectron spectroscopy.

Chemical groups	Binding energy (eV)	% Atomic
Graphitic / aromatic carbon (-C=C-)	284.1	9.78
Aliphatic carbon (-C-C-)	285.0	33.65
Epoxy/hydroxyl groups (C-O)	286.9	35.97
Carbon / ester (COO)	288.7	11.88
π- π * transition in aromatic	290.7	8.73

recommended by USEPA in order to simulate natural surface water. In this way, the medium exhibits characteristics of a real water environment where features of multiple salts coexist. Each ion in the medium affects nanomaterial aggregation and sedimentation behaviour.

Moreover, in the aquatic environment, the nanomaterial's stability can also be affected by interaction with Natural Organic Matter (NOM). It interacts with nanomaterial and increases the steric repulsive force between nanoparticles (Bundschuh et al., 2018). Consequently, the surface coating formed in nanoparticles can increase stability and its bioavailability (Jiang et al., 2017).

The dispersion stability of GO and the GO-AgNPs nanohybrid was studied in ultrapure water and a fish embryo medium in the presence and absence of NOM (Fig. 3-A, B). The GO and GO-AgNPs in ultrapure water feature desirable stability demonstrated by a small decrease in

absorbance (less than 20% for all samples) and a high surface charge ($\zeta_{GO} = -47{,}9 \pm 2{,}9$ mV and $\zeta_{GO\text{-}AgNPs} = -46{,}6 \pm 2{,}5$ mV) (OECD, 2017) (Fig. 3-C). This probably occurred due to high surface oxygen contents and small particle size. However, in the zebrafish embryo medium, after 24 h the samples decreased absorbance to less than 40% of the initial, and the surface charge reduced to $\zeta_{GO} = -24{,}8 \pm 2{,}2$ mV and $\zeta_{GO\text{-}AgNPs} = -18{,}8 \pm 0{,}7$ mV (Fig. 3-D). The lower colloidal stability was brought about by the ionic strength of medium and salt types (cationic salts like Na^{+}, Ca^{2+} e Mg^{2+}) that compete for adsorption with protons on the colloidal surface and reduced ionic strength (He et al., 2017). Consequently, aggregation and/or destabilization of flakes occur; it is possible to observe, however, nanomaterial floating, separating the dispersion into two phases as seen through a visual inspection (Fig. 3-B).

The presence of NOM has the potential to change stability due to hydrogen bonds, Lewis acid-base interactions, π– π interactions, and steric repulsions (Jiang et al., 2017). Similar to Clemente et al. (2017), an enhancement of colloidal stability in the presence of NOM was observed for GO in the zebrafish medium, which maintained ~90% initial absorbance throughout 72 h. However, the NOM at 20 mg mL^{-1} was not sufficient to produce stable dispersions for GO-AgNPs due to the lower amount of oxygen groups promoted by the partial reduction of graphene oxide caused by borohydride, as demonstrated by the lower surface charge (Zeta potential), XRD patterns and decrease of total percentage of C-O (High resolution C1s XPS spectra). In this way, the number of functional sites that NOM may interact with is not enough to enhance the colloidal stability of a nanohybrid in the fish embryo medium. However, it is very difficult to probe the stability of GO-based materials with much precision. Due to flocculent settling, the supernatant phase and the sedimentation/coagulation phase demonstrates different nanomaterial behaviours/concentrations. Thus, the collected material for the UV-Vis studied only reflects the condition of the upper layer (Fig. 3).

3.4. Toxicity on Zebrafish embryos

Chorion is a polypeptide structure that protects the embryo from exposure to external agents until hatching and represents a biological barrier to protect embryos. In this way, the effects observed after exposition are directly related to the permeability of chorion to this chemical compound (Henn and Braunbeck, 2011).

Protocols for chorion membrane removal are emerging to overcome this matter, and high throughput screening systems using embryos without chorion are already being exploited for nanomaterial toxicity studies (Pelka et al., 2017). Additionally, nanomaterial physicochemical properties might allow us to determine how it would interact with biological membranes, (i.e. chorion) and consequently, determine the effects observed in organisms (Paatero et al., 2017; Meng et al., 2018). Its removal seems to make the organism more susceptible. For example, (Olasagasti et al., 2014) observed the influence of chorion membrane in the deleterious exposition effects (i.e. changes in gene expression and in the uptake of NPs) of commercial AgNPs (18 mm) in zebrafish. When an embryo was surrounded by chorion (e.g. exposition begins with 4 hpf and finishes with 48 hpf), it did not show changes in comparison to the control. On the other hand, when the exposition started after hatching (72 hpf) they noted overexpression in Mt (considered as a specific biomarker for metal toxicity) and Il1β genes (that are activated in response to inflammation and involved in the innate immune response) and in the uptake of NPs after 48 h. Hatched embryos therefore provide an assessment potential of real toxic nanoparticle effects, without the influence of a chorion membrane. The ability of nanoparticles to

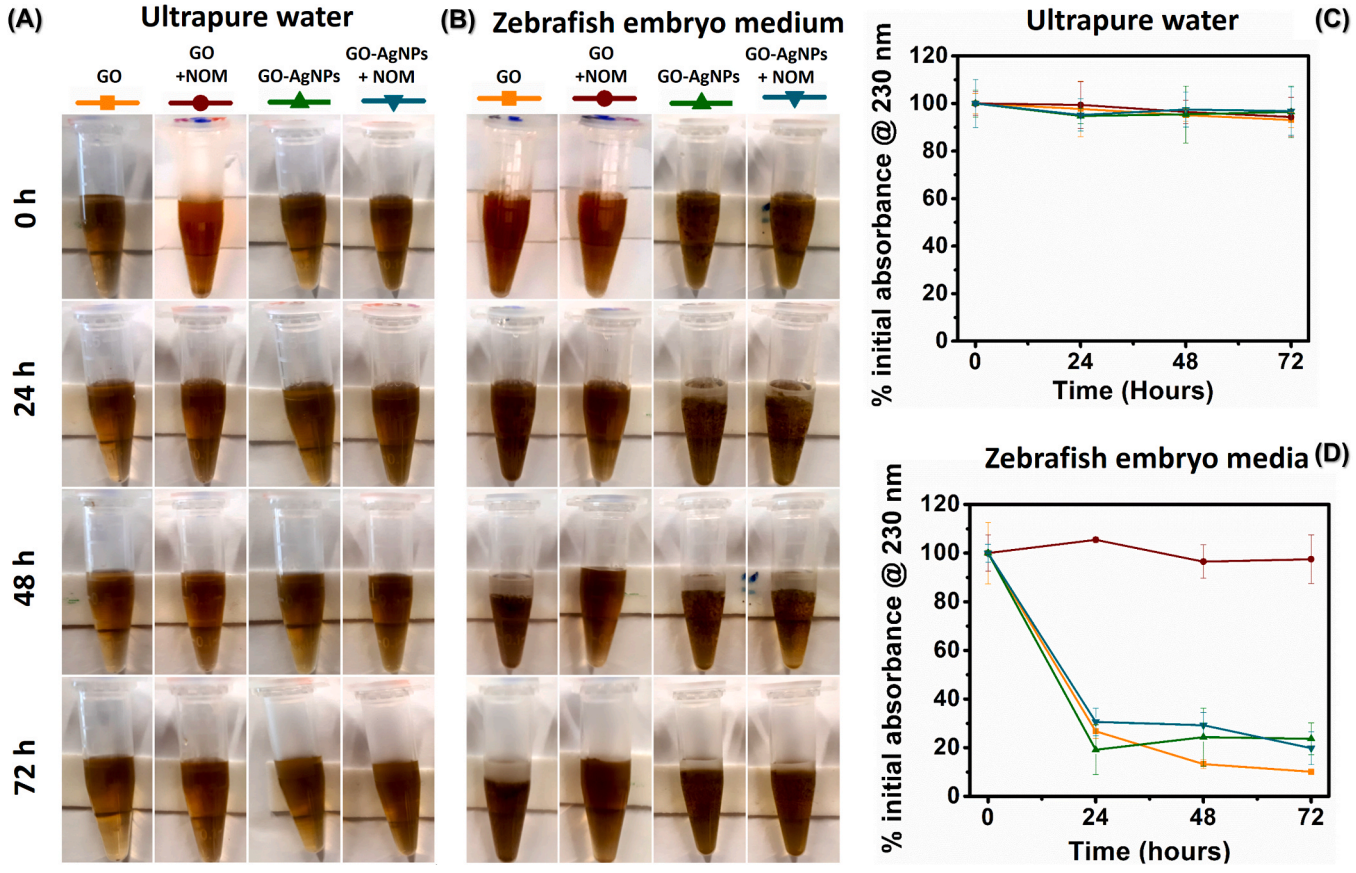

Fig. 3. Monitoring the dispersing stability of GO and GO-AgNPs in ultrapure water and Zebrafish embryo medium in the presence and absence of NOM (Final concentration: 20 mg L^{-1}). Visual inspection in ultrapure water (A) and fish embryo media (B) for 72 h. Percentage of initial absorbance @ 235 nm of samples at ultrapure water (C) and fish embryo media (D).

penetrate chorion then is a key factor in the experimental design that influences toxicology profiles (Paatero et al., 2017; Hamm et al., 2019). The chorion-off approach for the embryo toxicity assay was developed to ensure the contact of naked embryos with nanoparticles and eliminate differences with the chorion barrier (Panzica-Kelly et al., 2015). It is an important step in knowledge towards the development of nanosafety studies.

The exposure of $AgNO_3$ to chorionated and de-chorionated embryos results in LC_{50} values of 69.8 (61.1–78.8) and 38.1 (33.3–41.0) μg L^{-1}, respectively. LC_{50} in the presence of NOM reduced toxicity, changing

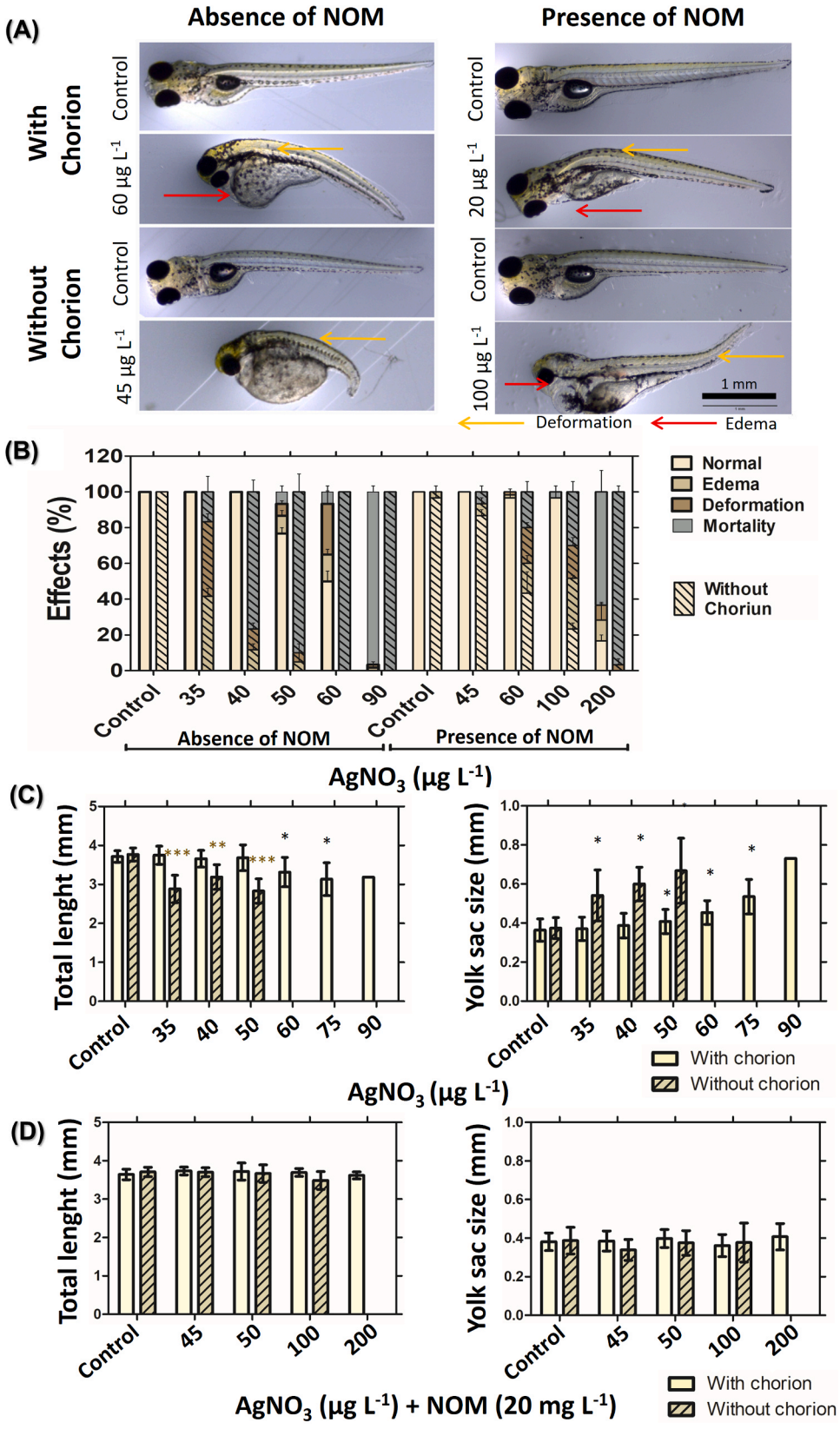

Fig. 4. Toxicity of $AgNO_3$ on zebrafish embryos in the presence and absence of NOM (20 mg L^{-1}). Visual inspection of larvae with 96 hpf (A). Deleterious effects (percentage) observed at final of exposure (B). Total length and yolk sac size for larvae exposure to $AgNO_3$ in absence of NOM (C). Total length and yolk sac size for larvae exposure to $AgNO_3$ in presence of NOM (D). Asterisks indicate groups that statistically differed from the control (one-way ANOVA, followed by Dunnet's: * $p < 0.05$, ** $p < 0.01$ and *** $p < 0.01$).

this to a higher value. In this case, the LC_{50} was 172.1 (162.1–183.6) and 94.0 (79.1–119.0) μg L^{-1} for exposition with and without chorion, respectively (Fig. 4). Survival embryos presented a bigger yolk sac size than the control for exposure to 50, 60, and 75 μg L^{-1}, and 35, 40, and 50 μg L^{-1} $AgNO_3$ (absence of NOM) for chorionated and de-chorionated embryos respectively (Fig. 4- C). This deleterious effect did not occur in larvae exposure to $AgNO_3$ in the presence of NOM (at 20 mg L^{-1}) (Fig. 4-D).

Considering LC_{50} values, the deleterious effects are more pronounced when embryos are de-chorionated and $AgNO_3$ exposure occurs in the absence of NOM. In the control group, all animals showed normal development. It is likely that the sulfhydryl groups present in the chorion were able to absorb cations, leading to low Ag^+ penetration into chorionic space.

These effects agree with those reported by Powers et al. (2010), who observed a small aggregation of chorion in embryos exposed to $AgNO_3$. Chorion might have been acting then as a major barrier to entry into the perivitelline space of metal cations (Burnison et al., 2006). The toxicological profiles of the nanoparticle might thus be influenced by surface charges; it would then modify the capacity to penetrate through biological barriers such as chorion (Paatero et al., 2017).

The physical deformities caused by the exposure of zebrafish embryos to AgNPs have already been reported (Lee et al., 2007; Asharani et al., 2008; Massarsky et al., 2013; Ribeiro et al., 2014; Cáceres-Vélez et al., 2018). It has also been documented that AgNPs can increase the production of reactive oxidative species (ROS) (Massarsky et al., 2013) and consequently, induce significant structural damage (Ale et al., 2018). Moreover, Ag^+ can cross the gill membrane and unbalance the ionoregulatory system because it replaces the Na^+ of the Na^+/K^+ATPase pump which is present in this organ (Kwok et al., 2016). Thus, this process has the potential to lead to the accumulation of fluid under the skin (edema).

Furthermore, NOM acted as a natural antidote for Ag^+. Ionic Ag was able to interact with NOM thought carboxylic groups and mitigated its deleterious effects on embryos (Gao et al., 2015). In this way, NOM may reduce toxicity because it can work as a free-radical scavenger.

The embryos exposed to GO (in the presence or absence of NOM) did not present any deleterious effects, although we were able to observe the presence of GO inside the digestive tract (Fig. 5-A) and in the gills (Fig. 5-B) of larvae as observed by Raman spectroscopy (Supplementary Material; Fig. S2). Through this technique, it is possible to see the D and G bands (signal spectra pattern characteristic of GO) inside the organism exposed, which confirms the internalization of carbon nanomaterial (Hu et al., 2015). Unfortunately, analysis for the bio-distribution of GO-AgNPs in the embryos through Raman spectroscopy was not possible due to the low concentration dose necessary to maintain the organism alive. Therefore, the nanohybrid was not sufficiently concentrated for Raman measurements to detect it.

Prior to 120 hpf, the embryos did not actively eat, but were able to start gaping from the protruding-mouth embryo stage (72 hpf) (Kimmel et al., 1995) allowing the accumulation of nanomaterial along the digestive tract. Moreover, the epidermal route (i.e. epidermis and gills) also plays an important role in the uptake and bio-distribution of nanoparticles (van Pomeren et al., 2017).

For the GO-AgNP hybrid, LC_{50} values for chorionated and de-chorionated embryos were, respectively, 1.4 (1.3–1.7) and 1.0 (0.9–1.2) mg L^{-1}. The presence of NOM rose to a higher value, indicating a mitigation of ecotoxicity. In this case, the LC_{50} was 2.3 (2.2–2.5) mg L^{-1} for chorionated embryos and 1.2 (1.1–1.4) mg L^{-1} for de-chorionated embryos (Fig. 6-A, B). The LC_{50} for all groups appears in Table 3, below.

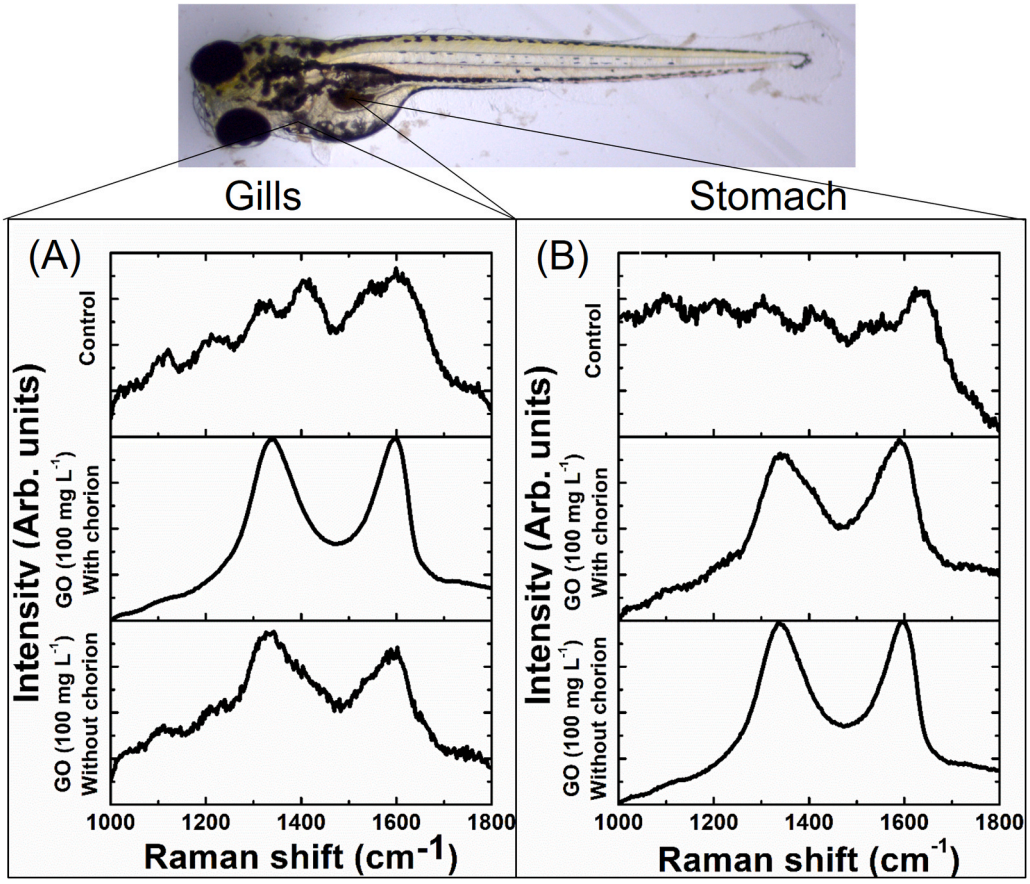

Fig. 5. Visual inspection of larvae with 96 hpf exposure to GO (100 mg L^{-1}) and the accumulation of nanomaterial as confirmed by Raman spectroscopy in gill (A) and stomach (B).

Deleterious effects for survival embryos (pericardial edema, notochord malformation as scoliosis, and shortened body) demonstrated the dose-dependent response for exposition to GO-AgNPs. At a higher GO-AgNP concentration, some embryos failed to absorb the yolk sac (Fig. 6- C-D). The lack of intake nutrients, then, may compromise the normal development of embryos.

The implications of NOM on the environmental risk assessment of nanomaterial and realistic exposure scenarios involve understanding NOM's environmental interactions and its influence on ecotoxicity (Castro et al., 2018). The nanomaterial can interact with organic ligands, thus forming a spontaneous molecular coating: the "NOM-corona" (Nasser and Lynch, 2016). NOM-coronas have the capacity to influence nanomaterial modification processes in the environment, including dissolution (for metallic nanoparticles), colloidal stability and bio-distribution (Clemente et al., 2017; Jiang et al., 2017; Baalousha et al., 2018; Cáceres-Vélez et al., 2018). Additionally, corona formation promotes a surface modification that alters the nano-bio-eco-interface, and provides a new biological and environmental entity for nanomaterial (Docter et al., 2015).

The presence of NOM might in fact modulate toxicity by adsorption on the AgNP surface, forming a corona that provides the reducing dissolution rates from AgNPs into Ag^+ (Gunsolus et al., 2015; Wang et al., 2016; Cáceres-Vélez et al., 2018), and consequently, could reduce ecotoxicity. Hence, the eco-toxicological profiles are determined by intrinsic features and by surrounding environmental conditions (Tortella et al., 2019). For this reason, many studies are considering this co-exposure scenario (nanoparticles + NOM) in order to reach more environmentally relevant scenarios (Chen et al., 2015; Gao et al., 2015; Clemente et al., 2017). The presence of NOM might be able to mediate the adsorption and reduction of free Ag^+ into AgNPs on the GO surface, thus generating a GO-AgNPs hybrid (Dong et al., 2019) and decreasing free silver ions in dissolution. Therefore, the amount of free silver ions may be said to affect bioavailability in aqueous media depending on the dissolution rate and adsorption processes of metal NPs (Wang et al., 2016).

As reported in the literature, the primary toxicity of AgNPs is caused by the release of silver ions, but is also influenced by the nanoparticles themselves (Van Aerle et al., 2013; Abramenko et al., 2018). Therefore, the dissolution of nanoparticles plays a pivotal role in metal nanoparticle fate, bio-distribution and toxicity and needs to be taken into consideration as a decision criterion in a regulatory context (Klaessig, 2018). In fact, there is a correlation between dissolution behaviour and the toxicity of AgNPs in different ionic environments, especially when mediated by the presence of chloride ions (Lee et al., 2018).

Furthermore, differences between observed exposure effects of GO-AgNPs nanohybrids and each nanomaterial isolated (GO and AgNPs) was also observed by (Wierzbicki et al., 2019). They observed an enhancement of antibacterial properties in the nanohybrids and an inhibition of AgNP toxic effects – such as cytotoxicity towards fibroblasts, human umbilical vein endothelial cells, and chicken embryo chorioallantois membranes. Similarly, they also demonstrated the good biocompatibility between GO and the nanohybrid GO-AgNPs.

In order to understand the effects from the dissolution of silver nanoparticles on toxicity, filtrate-only control was performed. The idea was to observe the potential effects of the remaining filtrates and assess the influence of dissolved ions in the ecotoxicity assay (Petersen, 2015). The filtrate-only control did not reveal any deleterious effects in chorionated embryos. Conversely, for embryo exposure without chorion, it was possible to observe an enhancement of impairment effects on development. However, it was not possible to calculate the LC_{50} value because it was higher than the maximum value studied (Supplementary Material, Fig.S3). According to this, the silver nanoparticle dissolution promoted low ion releases and the major cause of impairments observed in GO-AgNPs exposure seems to have been mainly produced by the nanohybrids themselves.

The XPS high-resolution spectra for Ag with GO-AgNPs after 72 h in the same conditions as those of the FET assay did not reveal any alteration in silver speciation at surface level in comparison to the control (Supplementary Material, Table 1 and Fig.S4). Similarly, Intrchom et al. (2018) observed a reduced dissolution in Ag^+ from carbon nanotube-AgNP nanohybrids, and consequently, a decline of ecotoxicity in freshwater algae (*Chlamydomonas reinhardtii*). Moreover, it is important to emphasize that the nanohybrid effects cannot have been attributed to AgNPs alone. In this case, a potentiation effect might have been present. For example, Liu et al. (2017) studied the impact of GO-AgNPs on bacterial biofilm formation. The inhibition was attributed to ROS formation and physical damage. The observed effect of the nanohybrid was stronger than that observed in a single exposure to GO or AgNPs. These findings reinforce the importance of studying the nanohybrid as a new material because the effect may be distinct from the isolated material.

It was not possible to evaluate the toxic effects of isolated AgNPs because it proved too challenging to synthesize nanoparticles in an aqueous solution with the same characteristics (e.g. shape, size, surface chemistry and structural defects). For example, De Faria et al. (2014) synthesized AgNPs anchored in GO-AgNPs and produced nanoparticles with an average size of 7.5 nm and spherical morphology. Whereas, in the absence of GO, the AgNPs produced showed variable shape and a bigger diameter (~ 60 nm). Further, the presence of GO in an aqueous solution modified the environment in which the reduction of Ag^+ would occur, and the presence of functional groups made an ideal scaffold grown from AgNPs, providing an anchor to begin nucleation and prevent aggregation (Perreault et al., 2015). Therefore, the presence of GO plays a pivotal role in the nucleation and growth of AgNPs, enabling the generation of smaller nanoparticles. A GO scaffold, then, is important for modifying the silver nanoparticles' toxic characteristics (Abramenko et al., 2018; George et al., 2012; Liu et al., 2019).

It is, in fact, very hard to establish a direct comparison among isolated materials and nanohybrids because their chemical and physical properties may be distinct one from the other. According to results in the literature, the LC_{50} for AgNPs ranges from 0.050 to 17 mg L^{-1} (Orbea et al., 2017; Boyle and Goss, 2018). Therefore, the immobilization of silver nanoparticles on a graphene oxide surface might decrease the adverse effects of AgNPs on zebrafish embryos as demonstrated by the higher LC_{50} value. Finally, in this work, the LC_{50} of $AgNO_3$ (69 μg L^{-1}) was 20 times less than the LC_{50} of GO-AgNPs (1.4 mg L^{-1}) under the same conditions (embryos with chorion and in the absence of NOM), demonstrating that a silver ionic is more toxic than a nanohybrid.

Overall, an important factor in our findings, which distinguishes the GO-AgNPs over isolated AgNPs, may be the reduction in the nanoparticles' dynamics, due to an attachment of the silver particle to the GO surface. This leads to a hybrid material with reduced dissolution behaviour and differentiated interaction with biological tissues, both having a critical impact on the toxicity of nanohybrids when compared with isolated AgNPs. However, one should pay attention to the fact that GOs present huge variability regarding their toxicological effects on zebrafish embryos, potentially leading to results very different from those found in our present assessment (d'Amora et al., 2017; Chen et al., 2017; Bangeppagari et al., 2019). Therefore, it is not possible to generalize the toxicological profile of GO-AgNPs hybrids for the moment. With this in mind, it is mandatory to provide a complete nanohybrid physicochemical characterization during toxicity testing, which should be geared towards future comparative studies and the harmonization of methodologies for the safe-by-design of various types of graphene-nanoparticles hybrid materials.

4. Conclusions

Herein, GO-AgNPs nanohybrid was synthesized through Ag^+ reducing to AgNPs, using $NaBH_4$ as reducing agent. In addition, the GO-AgNPs was well characterized, considering the requirements for nanotoxicology studies. The natural organic matter (20 mg L^{-1}) enhanced the

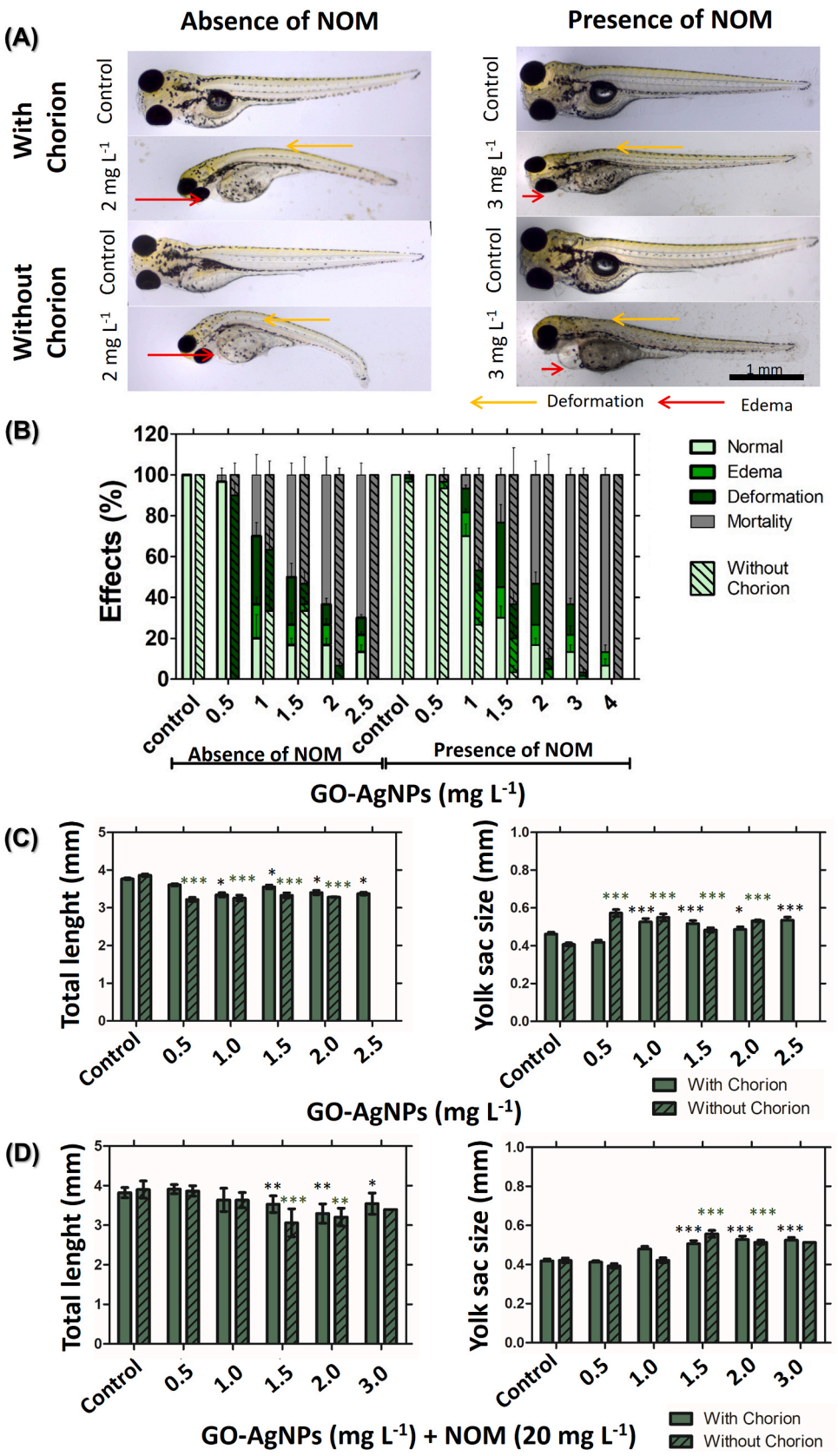

Fig. 6. Toxicity of GO-AgNPs on zebrafish embryos in the presence and absence of NOM (20 mg L^{-1}). Visual inspection of larvae with 96 hpf (A). Deleterious effects (percentage) observed at final of exposure (B). Total length and yolk sac size for larvae exposure to GO-AgNPs in absence of NOM (C). Total length and yolk sac size for larvae exposure to GO-AgNPs in presence of NOM (D). Asterisks indicate groups that statistically differed from the control (one-way ANOVA, followed by Dunnet's: * $p < 0.05$, ** $p < 0.01$ and *** $p < 0.01$).

Table 3
LC_{50} values (mg L^{-1}) for fish exposed to $AgNO_3$, GO and GO-AgNPs in the absence and presence of NOM (20 mg L^{-1}).

		Absence of NOM	Presence of NOM
With chorion	$AgNO_3$	0.069 (0.061 – 0.079)	0.172 (0.162 – 0.183)
	GO	>100	>100
	GO-AgNPs	1.4 (1.3 – 1.7)	2.3 (2.2 – 2.5)
Without chorion	$AgNO_3$	0.038 (0.033 – 0.041)	0.094 (0.079 – 0.119)
	GO	>100	>100
	GO-AgNPs	1.0 (0.9 – 1.2)	1.2 (1.1 – 1.4)

dispersion stability of GO in a zebrafish medium for up to 72 h, though this effect was not observed for GO-AgNPs. The ecotoxicity of $AgNO_3$ and the nanohybrid on zebrafish embryos was observed in a dose-response manner, in the presence and absence of chorion. GO did not affect the embryos with any toxicity, with or without chorion, even at a higher exposure concentration (100 mg L^{-1}); indicating that silver drives down toxicity in the nanohybrid. Furthermore, it was verified that the chorion embryo membrane critically influences toxicity. NOM mitigated the ecotoxicity effect of Ag^{+} and GO-AgNPs on the embryos, suggesting implications for risk assessment involving these materials. The biocompatibility of GO and the inhibition of silver dissolution, as observed in the filtrate-only control, both suggest that GO may acts as a platform for the reduction of silver toxicity.

In light of the above, this work is an important contribution toward proactive ecotoxicological evaluation involving the emerging nano-hybrid materials. Finally, the approach used for chorion membrane removal guarantees the direct exposure of embryos, reducing the sources of variability and contributing to the standardization of fish embryo toxicity testing.

CRediT authorship contribution statement

Aline M.Z. de Medeiros: Conceptualization, Methodology, Investigation, Data curation, Writing - original draft preparation, Project Administration. **Diego Stéfani T. Martinez**: Conceptualization, Methodology, Validation, Writing - review and editing, Supervision. **Gabriela H. da Silva**: Methodology, Investigation. **Latif U. Khan**: Investigation. **Carlos A. Ospina**: Investigation. **Vera Lúcia de Castro**: Validation, Writing - review & editing. **Oswaldo L. Alves**: Validation, Funding acquisition. **Diego Stéfani T. Martinez**: Conceptualization, Methodology, Validation, Writing - review & editing, Supervision, Funding acquisition. All authors have read and agreed to the published version of the manuscript.

Declaration of Competing Interest

The authors declare that they have no known competing financial interests or personal relationships that could have appeared to influence the work reported in this paper.

Acknowledgments

The Coordenação de Aperfeiçoamento de Pessoal de Nível Superior – Brasil (CAPES / Brasil) – Finance Code 001, the National Council of Scientific and Technological Development (CNPq / Brasil - Grant 169984/2018-4) and the São Paulo Research Foundation (FAPESP) supported this study. The authors are grateful to CNPEM facilities (LME, AFM, XPS, LAM, Raman and Nanotox), INCT-Inomat, the AgroNano Network, the Brazil-China Centre for Research and Innovation in Nanotechnology (CBC-Nano / Brasil) and the National System of Laboratories in Nanotechnologies (SisNANO/MCTIC / Brasil). DSTM thanks the CNPq / Brasil to the Research Productivity Fellowship grant (Proc. No. 313494/2017-7).

Appendix A. Supporting information

Supplementary data associated with this article can be found in the online version at doi:10.1016/j.ecoenv.2020.111776.

References

Abramenko, N.B., Demidova, T.B., Abkhalimov, EV., Ershov, B.G., Krysanov, E.Y., Kustov, L.M., 2018. Ecotoxicity of different-shaped silver nanoparticles: case of zebrafish embryos. J. Hazard. Mater. 347, 89–94. https://doi.org/10.1016/j.jhazmat.2017.12.060.

Ahmad, N., Al-Fatesh, A.S., Wahab, R., Alam, M., Fakeeha, A.H., 2020. Synthesis of silver nanoparticles decorated on reduced graphene oxide nanosheets and their electrochemical sensing towards hazardous 4-nitrophenol. J. Mater. Sci. Mater. Electron. 31, 11927–11937. https://doi.org/10.1007/s10854-020-03747-3.

Ale, A., Bacchetta, C., Rossi, A.S., Galdopórpora, J., Desimone, M.F., de la Torre, F.R., Gervasio, S., Cazenave, J., 2018. Ecotoxicology and environmental safety nanosilver toxicity in gills of a neotropical fi sh: metal accumulation, oxidative stress, histopathology and other physiological effects. Ecotoxicol. Environ. Saf. 148, 976–984. https://doi.org/10.1016/j.ecoenv.2017.11.072.

Asharani, P.V., Lian, Wu.Y., Gong, Z., Valiyaveettil, S., 2008. Toxicity of silver nanoparticles in zebrafish models. Nanotechnology 19, 255102. https://doi.org/10.1088/0957-4484/19/25/255102.

Baalousha, M., Afshinnia, K., Guo, L., 2018. Natural organic matter composition determines the molecular nature of silver nanomaterial-NOM corona. Environ. Sci. Nano 5, 868–881. https://doi.org/10.1039/c8en00018b.

Bangeppagari, M., Park, S.H., Kundapur, R.R., Lee, S.J., 2019. Graphene oxide induces cardiovascular defects in developing zebrafish (Danio rerio) embryo model: in-vivo toxicity assessment. Sci. Total Environ. 673, 810–820. https://doi.org/10.1016/j.scitotenv.2019.04.082.

Becerril, H.A., Mao, J., Liu, Z., Stoltenberg, R.M., Bao, Z., Chen, Y., 2008. Evaluation of solution-processed reduced graphene oxide films as transparent conductors. ACS Nano 2, 463–470. https://doi.org/10.1021/nn700375n.

Boyle, D., Goss, G.G., 2018. Effects of silver nanoparticles in early life-stage zebrafish are associated with particle dissolution and the toxicity of soluble silver. NanoImpact 12, 1–8. https://doi.org/10.1016/j.impact.2018.08.006.

Bundschuh, M., Filser, J., Lüderwald, S., Mckee, M.S., Metreveli, G., Schaumann, G.E., et al., 2018. Nanoparticles in the environment : where do we come from , where do we go to ? Environ. Sci. Eur. 30 https://doi.org/10.1186/s12302-018-0132-6.

Burnison, B.K., Meinelt, T., Playle, R., Pietrock, M., Wienke, A., Steinberg, C.E.W., 2006. Cadmium accumulation in zebrafish (Danio rerio) eggs is modulated by dissolved organic matter (DOM). Aquat. Toxicol. 79, 185–191. https://doi.org/10.1016/j.aquatox.2006.06.010.

Cáceres-Vélez, P.R., Fascineli, M.L., Sousa, M.H., Grisolia, C.K., Yate, L., de Souza, P.E.N., Estrela-Lopis, I., Moya, S., Azevedo, R.B., 2018. Humic acid attenuation of silver nanoparticle toxicity by ion complexation and the formation of a Ag 3+ coating. J. Hazard. Mater. 353, 173–181. https://doi.org/10.1016/j.jhazmat.2018.04.019.

Castro, V.L., Clemente, Z., Jonsson, C., Silva, M., Vallim, J.H., de Medeiros, A.M.Z., Martinez, D.S.T., 2018. Nanoecotoxicity assessment of graphene oxide and its relationship with humic acid. Environ. Toxicol. Chem. 37, 1998–2012. https://doi.org/10.1002/etc.4145.

Chakraborty, C., Sharma, A.R., Sharma, G., Lee, S.S., 2016. Zebrafish: a complete animal model to enumerate the nanoparticle toxicity. J. Nanobiotechnol. 14, 1–13. https://doi.org/10.1186/s12951-016-0217-6.

Chen, F., Hableel, G., Zhao, E., Jokerst, J.V., 2018. Multifunctional nanomedicine with silica: role of silica in nanoparticles for theranostic, imaging, and drug monitoring. J. Colloid Interface Sci. 521, 261–279. https://doi.org/10.1016/j.jcis.2018.02.053.

Chen, J., Sun, L., Cheng, Y., Lu, Z., Shao, K., Li, T., Hu, C., Han, H., 2016. Graphene oxide-silver nanocomposite: novel agricultural antifungal agent against fusarium graminearum for crop disease prevention. ACS Appl. Mater. Interfaces 8, 24057–24070. https://doi.org/10.1021/acsami.6b05730.

Chen, F.Y., Li, N., Hsueh, J.F., Huang, C.C., Lu, F.I., Fu, T.F., Yan, S.J., Lee, Y.H., Wang, Y.J., 2020. International Journal of Molecular Sciences 21 (8). https://doi.org/10.3390/ijms21082864.

Chen, Y., Ren, C., Ouyang, S., Hu, X., Zhou, Q., 2015. Mitigation in multiple effects of graphene oxide toxicity in zebrafish embryogenesis driven by humic acid. Environ. Sci. Technol. 49, 10147–10154.

Chen Y., Hu X., Sun J., Zhou Q., Chen Y., Hu X., et al. Specific nanotoxicity of graphene oxide during zebrafish embryogenesis Specific nanotoxicity of graphene oxide during zebrafish embryogenesis, 2017;5390. doi:⟨10.3109/17435390.2015.1005032⟩.

Çiplak, Z., Yildiz, N., Cąlimli, A., 2015. Investigation of graphene/Ag nanocomposites synthesis parameters for two different synthesis methods. Fuller. Nanotub Carbon Nanostruct. 23, 361–370. https://doi.org/10.1080/1536383X.2014.894025.

Clemente, Z., VLSS, Castro, Franqui, L.S., Silva, C.A., Martinez, D.S.T., 2017. Nanotoxicity of graphene oxide: assessing the influence of oxidation debris in the presence of humic acid. Environ. Pollut. 225, 118–128. https://doi.org/10.1016/j.envpol.2017.03.033.

d'Amora, M., Camisasca, A., Lettieri, S., Giordani, S., 2017. Toxicity assessment of carbon nanomaterials in zebrafish during development. Nanomaterials 7, 414. https://doi.org/10.3390/nano7120414.

Das, M.R., Sarma, R.K., Saikia, R., Kale, V.S., Shelke, M.V., Sengupta, P., 2011. Synthesis of silver nanoparticles in an aqueous suspension of graphene oxide sheets and its

antimicrobial activity. Colloids Surf. B Biointerfaces 83, 16–22. https://doi.org/10.1016/j.colsurfb.2010.10.033.
De Faria, A.F., Martinez, D.S.T., Meira, S.M.M., de Moraes, A.C.M., Brandelli, A., Filho, A.G.S., Alves, O.L., 2014. Anti-adhesion and antibacterial activity of silver nanoparticles supported on graphene oxide sheets. Colloids Surf. B Biointerfaces 113, 115–124. https://doi.org/10.1016/j.colsurfb.2013.08.006.
De Luna, L.A.V., de Moraes, A.C.M., Consonni, S.R., Pereira, C.D., Cadore, S., Giorgio, S., Alves, O.L., 2016. Comparative in vitro toxicity of a graphene oxide - silver nanocomposite and the pristine counterparts toward macrophages. J. Nanobiotechnol. 14, 12 https://doi.org/10.1186/s12951-016-0165-1.
De Moraes, A.C.M., 2015. Graphene oxide-silver nanocomposite as a promising biocidal agent against methicillin- resistant Staphylococcus aureus. Int. J. Nanomed. 10, 6847–6861.
Dideikin, A.T., Vul, A.Y., 2019. Graphene oxide and derivatives: the place in graphene family. Front Phys. 6, 6 https://doi.org/10.3389/fphy.2018.00149.
Docter, D., Westmeier, D., Markiewicz, M., Stolte, S., Knauer, S.K., Stauber, R.H., 2015. The nanoparticle biomolecule corona: lessons learned - challenge accepted? Chem. Soc. Rev. 44, 6094–6121. https://doi.org/10.1039/c5cs00217f.
Dong, B., Liu, G., Zhou, J., Wang, J., Jin, R., Zhang, Y., 2019. Effects of reduced graphene oxide on humic acid-mediated transformation and environmental risks of silver ions. J. Hazard Mater. 385, 121597. https://doi.org/10.1016/j.jhazmat.2019.121597.
Dresselhaus, M.S., Jorio, A., Hofmann, M., Dresselhaus, G., Saito, R., 2010. Perspectives on carbon nanotubes and graphene Raman spectroscopy. Nano Lett. 10, 751–758. https://doi.org/10.1021/nl904286r.
Encarnacion-Rosado, J., Garcia-pabon, K., Villalobos-santos, J.C., Makarov, V.I., Avalos, J.A., Weiner, B.R., et al., 2016. Improving Cytotoxicity Against Cancer Cells by Chemo-photodynamic Combined Modalities using Silver-graphene Quantum Dots Nanocomposites. Int. J. Nanomedicine 11, 107. https://doi.org/10.2147/IJN.S95440.
Fadeel, B., Bussy, C., Merino, S., Vázquez, E., Flahaut, E., Mouchet, F., Evariste, L., Gauthier, L., Koivisto, A.J., Vogel, U., Martín, C., Delogu, L.G., Buerki-Thurnherr, T., Wick, P., Beloin-Saint-Pierre, D., Hischier, R., Pelin, M., Candotto Carniel, F., Tretiach, M., Cesca, F., Benfenati, F., Scaini, D., Ballerini, L., Kostarelos, K., Prato, M., Bianco, A., 2018. Safety assessment of graphene-based materials: focus on human health and the environment. ACS Nano 12, 10582–10620. https://doi.org/10.1021/acsnano.8b04758.
Faria, A.F., Martinez, D.S.T., Moraes, A.C.M., Maia Da Costa, M.E.H., Barros, E.B., Souza Filho, A.G., Paula, A.J., Alves, O.L., 2012. Unveiling the role of oxidation debris on the surface chemistry of graphene through the anchoring of ag nanoparticles. Chem. Mater. 24, 4080–4087. https://doi.org/10.1021/cm301939s.
Fonseca, L.C., de Araújo, M.M., de Moraes, A.C.M., da Silva, D.S., Ferreira, A.G., Franqui, L.S., Martinez, D.S.T., Alves, O.L., 2018. Nanocomposites based on graphene oxide and mesoporous silica nanoparticles: Preparation, characterization and nanobiointeractions with red blood cells and human plasma proteins. Appl. Surf. Sci. 437, 110–121. https://doi.org/10.1016/j.apsusc.2017.12.082.
Gao, J., Powers, K., Wang, Y., Zhou, H., Roberts, S.M., Moudgil, B.M., Koopman, B., Barber, D.S., 2015. Influence of Suwannee River humic acid on particle properties and toxicity of silver nanoparticles. Chemosphere 89, 96–101. https://doi.org/10.1016/j.chemosphere.2012.04.024.
George S., Lin Sijie, Ji Z., Thomas CR, Li L., Mecklenburg M., et al. Surface Defects on Plate-Shaped Silver Nanoparticles Contribute to Its Hazard Potential in a Fish Gill Cell Line and Zebra fi sh Embryos 2012:3745–3759. doi:10.1021/nn204671v.
Grillo, R., Rosa, A.H., Fraceto, L.F., 2015. Engineered nanoparticles and organic matter: a review of the state-of-the-art. Chemosphere 119, 608–619. https://doi.org/10.1016/j.chemosphere.2014.07.049.
Gunsolus, I.L., Mousavi, M.P.S., Hussein, K., Bühlmann, P., Haynes, C.L., 2015. Effects of humic and fulvic acids on silver nanoparticle stability, dissolution, and toxicity. Environ. Sci. Technol. 49, 8078–8086. https://doi.org/10.1021/acs.est.5b01496.
Hamm, J.T., Ceger, P., Allen, D., Stout, M., Maull, E.A., Baker, G., et al., 2019. Characterizing sources of variability in zebrafish embryo screening protocols. ALTEX 36, 103–120. https://doi.org/10.14573/altex.1804162.
Haque, E., Ward, A.C., 2018. Zebrafish as a model to evaluate nanoparticle toxicity. Nanomaterials 8, 1–18. https://doi.org/10.3390/nano8070561.
Hassandoost, R., Pouran, S.R., Khataee, A., Orooji, Y., Joo, S.W., 2019. Hierarchically structured ternary heterojunctions based on Ce3+/ Ce4+ modified Fe3O4 nanoparticles anchored onto graphene oxide sheets as magnetic visible-light-active photocatalysts for decontamination of oxytetracycline. J. Hazard. Mater. 376, 200–211. https://doi.org/10.1016/j.jhazmat.2019.05.035.
He, K., Chen, G., Zeng, G., Peng, M., Huang, Z., Shi, J., Huang, T., 2017. Stability, transport and ecosystem effects of graphene in water and soil environments. Nanoscale 9, 5370–5388. https://doi.org/10.1039/C6NR09931A.
He, Y., Peng, G., Jiang, Y., Zhao, M., Wang, X., Chen, M., Lin, S., 2020. Environmental hazard potential of nano-photocatalysts determined by nano-bio interactions and exposure conditions. Small 16, 1–8. https://doi.org/10.1002/smll.201907690.
Henn, K., Braunbeck, T., 2011. Dechorionation as a tool to improve the fish embryo toxicity test (FET) with the zebrafish (Danio rerio). Comp. Biochem. Physiol. C Toxicol. Pharm. 153, 91–98. https://doi.org/10.1016/j.cbpc.2010.09.003.
Hoa, L.T., Linh, N.T.Y., Chung, J.S., Hur, S.H., 2017. Green synthesis of silver nanoparticle-decorated porous reduced graphene oxide for antibacterial non-enzymatic glucose sensors. Ion. Kiel. 23, 1525–1532. https://doi.org/10.1007/s11581-016-1954-0.
Hu, X., Ouyang, S., Mu, L., An, J., Zhou, Q., 2015. Effects of graphene oxide and oxidized carbon nanotubes on the cellular division, microstructure, uptake, oxidative stress, and metabolic profiles. Environ. Sci. Technol. 49, 10825–10833. https://doi.org/10.1021/acs.est.5b02102.
Hutchison, J.E., 2016. The road to sustainable nanotechnology: challenges, progress and opportunities. ACS Sustain. Chem. Eng. 4, 5907–5914. https://doi.org/10.1021/acssuschemeng.6b02121.
Intrchom, W., Thakkar, M., Hamilton, R.F., Holian, A., Mitra, S., 2018. Effect of carbon nanotube-metal hybrid particle exposure to freshwater algae chlamydomonas reinhardtii. Sci. Rep. 8, 15301. https://doi.org/10.1038/s41598-018-33674-7.
Janknecht, P., Proenc, F., Rodrigues, A., 2009. Quantification of humic acids in surface water: effects of divalent cations. J. Environ. Monit. 11, 377–382. https://doi.org/10.1039/b811942b.
Jiang, Y., Raliya, R., Liao, P., Biswas, P., Fortner, J.D., 2017. Graphene oxides in water: assessing stability as a function of material and natural organic matter properties. Environ. Sci. Nano 4, 1484–1493. https://doi.org/10.1039/c7en00220c.
Kavinkumar, T., Manivannan, S., 2016. Uniform decoration of silver nanoparticle on exfoliated graphene oxide sheets and its ammonia gas detection. Ceram. Int. 42, 1769–1776. https://doi.org/10.1016/j.ceramint.2015.09.138.
Kellici S., Acord J., Vaughn A., Power NP, Morgan DJ, Heil T. Calixarene Assisted Rapid Synthesis of Silver-Graphene Nanocomposites with Enhanced Antibacterial Activity, 2016. doi:10.1021/acsami.6b06052.
Khan, L.U., Silva, G.H., Medeiros, A.M.Z., Khan, Z.U., Gidlund, M., Brito, H.F., Moscoso-Londoño, O., Muraca, D., Knobel, M., Perez, C.A., Martinez, D.S.T., 2019. Fe3O4@SiO2 nanoparticles concurrently coated with chitosan and gdof:ce3+,tb3+ luminophore for bioimaging: toxicity evaluation in the zebrafish model. ACS Appl. Nano Mater. 2:6, 3114–3425 doi.org/10.1021/acsanm.9b00339.
Kim, M.J., Ko, D., Ko, K., Kim, D., Lee, J.Y., Woo, S.M., Kim, W., Chung, H., 2018. Effects of silver-graphene oxide nanocomposites on soil microbial communities. J. Hazard. Mater. 346, 93–102. https://doi.org/10.1016/j.jhazmat.2017.11.032.
Kimmel, C.B., Ballard, W.W., Kimmel, S.R., Ullmann, B., Schilling, T.F., 1995. Stages of embryonic development of the zebrafish. Dev. Dyn. an Off Public 203, 253–310. https://doi.org/10.1002/aja.1002030302.
Klaessig, F.C., 2018. Dissolution as a paradigm in regulating nanomaterials. Environ. Sci. Nano 5, 1070–1077. https://doi.org/10.1039/c7en01130j.
Koushik, D., Sen, S., Maliyekkal, S.M., Pradeep, T., 2016. Rapid dehalogenation of pesticides and organics at the interface of reduced graphene oxide – silver nanocomposite. J. Hazard. Mater. 308, 192–198. https://doi.org/10.1016/j.jhazmat.2016.01.004.
Kundu, N., Mukherjee, D., Maiti, T.K., Sarkar, N., 2017. Protein-guided formation of silver nanoclusters and their assembly with graphene oxide as an improved bioimaging agent with reduced toxicity. J. Phys. Chem. Lett. 8, 2291–2297. https://doi.org/10.1021/acs.jpclett.7b00600.
Kwok, K.W.H., Dong, W., Marinakos, S.M., Liu, J., Chilkoti, A., Wiesner, M.R., Chernick, M., Hinton, D.E., 2016. Silver nanoparticle toxicity is related to coating materials and disruption of sodium concentration regulation. Nanotoxicology 10, 1306–1317. https://doi.org/10.1080/17435390.2016.1206150.
Lee, K.J., Nallathamby, P.D., Browning, L.M., Osgood, C.J., Nancy, Xu.X.H., 2007. In vivo imaging of transport and biocompatibility of single silver nanoparticles in early development of zebrafish embryos. ACS Nano 1, 133–143. https://doi.org/10.1021/nn700048y.
Lee, K.Y., Jang, G.H., Byun, C.H., Jeun, M., Searson, P.C., Hyi, K., 2017. Zebrafish models for functional and toxicological screening of nanoscale drug delivery systems. : Promot. Preclin. Appl. 0, 1–13. https://doi.org/10.1042/BSR20170199.
Lee, W., Kim, E., Cho, H.J., Kang, T., Kim, B., Kim, M., Kim, Y., Song, N., Lee, J.S., Jeong, J., 2018. The relationship between dissolution behavior and the toxicity of silver nanoparticles on zebrafish embryos in different ionic environments. Nanomaterials 8, 652. https://doi.org/10.3390/nano8090652.
Li, J., Kuang, D., Feng, Y., Zhang, F., Xu, Z., 2013. Biosensors and bioelectronics green synthesis of silver nanoparticles – graphene oxide nanocomposite and its application in electrochemical sensing of tryptophan. Biosens. Bioelectron. 42, 198–206. https://doi.org/10.1016/j.bios.2012.10.029.
Lin, S., Yu, T., Yu, Z., Hu, X., Yin, D., 2018. Nanomaterials safer-by-design: an environmental safety perspective. Adv. Mater. 30, 1–5. https://doi.org/10.1002/adma.201705691.
Liu, C., Shen, J., Yeung, K.W.K., Tjong, S.C., 2017. Development and antibacterial performance of novel polylactic acid-graphene oxide-silver nanoparticle hybrid nanocomposite mats prepared by electrospinning (acsbiomaterials). ACS Biomater. Sci. Eng. 3, 471–486. https://doi.org/10.1021/acsbiomaterials.6b00766.
Liu, H., Wang, X., Wu, Y., Hou, J., Zhang, S., Zhou, N., Wang, X., 2019. Toxicity responses of different organs of zebrafish (Danio rerio) to silver nanoparticles with different particle sizes and surface coatings. Environ. Pollut. 246, 414–422. https://doi.org/10.1016/j.envpol.2018.12.034.
Lowry, G.V., Gregory, K.B., Apte, S.C., Lead, J.R., 2014. Transformations of nanomaterials in the environment. Front Nanosci. 7, 55–87. https://doi.org/10.1016/B978-0-08-099408-6.00002-5.
Mahmoudi, E., Ng, L.Y., Ba-Abbad, M.M., Mohammad, A.W., 2015. Novel nanohybrid polysulfone membrane embedded with silver nanoparticles on graphene oxide nanoplates. Chem. Eng. J. 277, 1–10. https://doi.org/10.1016/j.cej.2015.04.107.
Markiewicz, M., Kumirska, J., Lynch, I., Matzke, M., Köser, J., Bemowsky, S., Docter, D., Stauber, R., Westmeier, D., Stolte, S., 2018. Changing environments and biomolecule coronas: consequences and challenges for the design of environmentally acceptable engineered nanoparticles. Green. Chem. 20, 4133–4168. https://doi.org/10.1039/C8GC01171K.
Massarsky, A., Dupuis, L., Taylor, J., Eisa-Beygi, S., Strek, L., Trudeau, V.L., Moon, T.W., 2013. Assessment of nanosilver toxicity during zebrafish (Danio rerio) development. Chemosphere 92, 59–66. https://doi.org/10.1016/j.chemosphere.2013.02.060.
McGillicuddy, E., Murray, I., Kavanagh, S., Morrison, L., Fogarty, A., Cormican, M., Dockery, P., Prendergast, M., Rowan, N., Morris, D., 2017. Silver nanoparticles in the

environment: sources, detection and ecotoxicology. Sci. Total Environ. 575, 231–246. https://doi.org/10.1016/j.scitotenv.2016.10.041.
Meng, H., Leong, W., Leong, K.W., Chen, C., Zhao, Y., 2018. Biomaterials walking the line: the fate of nanomaterials at biological barriers. Biomaterials 174, 41–53. https://doi.org/10.1016/j.biomaterials.2018.04.056.
Mottier, A., Mouchet, F., Pinelli, É., Gauthier, L., Flahaut, E., 2017. Environmental impact of engineered carbon nanoparticles: from releases to effects on the aquatic biota. Curr. Opin. Biotechnol. 46, 1–6. https://doi.org/10.1016/j.copbio.2016.11.024.
Nazari, F., Movafeghi, A., 2018. Synthesis of reduced graphene oxide-silver nanocomposites and assessing their toxicity on the green Microalga chlorella vulgaris. Bionanoscience 8, 997–1007. https://doi.org/10.1007/s12668-018-0561-0.
OECD, 2013. OEcd guidelines for the testing of chemicals, section 2: effects on biotic systems!Test no. 236: fish embryo acute toxicity (fet) test. Organ Econ. Co. Oper. Dev. Paris 1–22. https://doi.org/10.1787/9789264203709-en.
OECD, 2017. Dispersion stability of nanomaterials in simulated environmental media. OECD Guide Test. Chem. 1–4. https://doi.org/10.1787/9789264067394-eng.
Olasagasti, M., Gatti, A.M., Capitani, F., Barranco, A., Pardo, M.A., Escuredo, K., et al., 2014. Toxic effects of colloidal nanosilver in zebrafish embryos. J. Appl. Toxicol. 34, 562–575. https://doi.org/10.1002/jat.2975.
Orbea, A., González-Soto, N., Lacave, J.M., Barrio, I., Cajaraville, M.P., 2017. Developmental and reproductive toxicity of PVP/PEI-coated silver nanoparticles to zebrafish. Comp. Biochem. Physiol. Part C. Toxicol. Pharm. 199, 59–68. https://doi.org/10.1016/j.cbpc.2017.03.004.
Paatero, I., Casals, E., Niemi, R., Özliseli, E., Rosenholm, J.M., 2017. Analyses in zebrafish embryos reveal that nanotoxicity profiles are dependent on surface-functionalization controlled penetrance of biological membranes. Sci. Rep. 7, 1–13. https://doi.org/10.1038/s41598-017-09312-z.
Panzica-Kelly, J.M., Zhang, C.X., Augustine-Rauch, K.A., 2015. Optimization and performance assessment of the chorion-off [Dechorinated] Zebrafish Developmental toxicity assay. Toxicol Sci 146, 127–134. https://doi.org/10.1093/toxsci/kfv076.
Park, M.V.D.Z., Bleeker, E.A.J., Brand, W., Cassee, F.R., Van Elk, M., Gosens, de Jong, W. H., Meesters, J., Peijnenburg, W., Quik, J., Vandebriel, R.J., Sips, A., 2017. I Considerations for safe innovation: the case of graphene. ACS Nano 11, 9574–9593. https://doi.org/10.1021/acsnano.7b04120.
Pasricha, R., Gupta, S., Srivastava, A.K., 2009. A facile and novel synthesis of Ag-graphene-based nanocomposites. Small 5, 2253–2259. https://doi.org/10.1002/smll.200900726.
Pelka, K.E., Henn, K., Keck, A., Sapel, B., Braunbeck, T., 2017. Size does matter – determination of the critical molecular size for the uptake of chemicals across the chorion of zebrafish (Danio rerio) embryos. Aquat. Toxicol. 185, 1–10. https://doi.org/10.1016/j.aquatox.2016.12.015.
Perreault, F., Fonseca De Faria, A., Elimelech, M., 2015. Environmental applications of graphene-based nanomaterials. Chem. Soc. Rev. 44, 5861–5896. https://doi.org/10.1039/c5cs00021a.
Petersen, E.J., 2015. Control experiments to avoid artifacts and misinterpretations in nanoecotoxicology testing NIST special publication 1200-11 control experiments to avoid artifacts and misinterpretations in nanoecotoxicology testing. NIST Spec. Publ. 1200. https://doi.org/10.6028/NIST.SP.1200-1.
Plazas-Tuttle, J., Rowles, L., Chen, H., Bisesi, J., Sabo-Attwood, T., Saleh, N., 2015. Dynamism of stimuli-responsive nanohybrids: environmental implications. Nanomaterials 5, 1102–1123. https://doi.org/10.3390/nano5021102.
Powers, C.M., Yen, J., Linney, E.A., Seidler, F.J., Slotkin, T.A., 2010. Silver exposure in developing zebrafish (Danio rerio): persistent effects on larval behavior and survival. Neurotoxicol. Teratol. 32, 391–397. https://doi.org/10.1016/j.ntt.2010.01.009.
Ren, W., Cheng, H.M., 2014. The global growth of graphene. Nat. Nanotechnol. 9, 726–730. https://doi.org/10.1038/nnano.2014.229.
Ribeiro, F., Gallego-Urrea, J.A., Jurkschat, K., Crossley, A., Hassellöv, M., Taylor, C., Soares, A.M.V.M., Loureiro, S., 2014. Silver nanoparticles and silver nitrate induce high toxicity to Pseudokirchneriella subcapitata, Daphnia magna and Danio rerio. Sci. Total Environ. 466–467, 232–241. https://doi.org/10.1016/j.scitotenv.2013.06.101.
Saleh, N., Afrooz, A., Bisesi Jr., J., Aich, N., Plazas-Tuttle, J., Sabo-Attwood, T., 2014. Emergent properties and toxicological considerations for nanohybrid materials in aquatic systems. Nanomaterials 4, 372–407. https://doi.org/10.3390/nano4020372.
Saleh, N.B., Aich, N., Plazas-Tuttle, J., Lead, J.R., Lowry, G.V., 2015. Research strategy to determine when novel nanohybrids pose unique environmental risks. Environ. Sci. Nano 2, 11–18. https://doi.org/10.1039/C4EN00104D.
Shao, W., Liu, X., Min, H., Dong, G., Feng, Q., Zuo, S., 2015. Preparation, characterization, and antibacterial activity of silver nanoparticle-decorated graphene oxide nanocomposite. ACS Appl. Mater. Interfaces 7, 6966–6973. https://doi.org/10.1021/acsami.5b00937.
Sharma, S., Prakash, V., Mehta, S.K., 2017. Graphene/silver nanocomposites-potential electron mediators for proliferation in electrochemical sensing and SERS activity. TrAC Trends Anal. Chem. 86, 155–171. https://doi.org/10.1016/j.trac.2016.10.004.
Sieber, S., Grossen, P., Bussmann, J., Campbell, F., Kros, A., Witzigmann, D., Huwyler, J., 2019. Zebrafish as a preclinical in vivo screening model for nanomedicines. Adv. Drug Deliv. Rev. 151–152, 152–168. https://doi.org/10.1016/j.addr.2019.01.001.
Sijie, Lin, Zhao, Y., Nel, A.E., Lin, Shuo, Zebrafi, sh, 2013. Zebrafish: an in vivo model for nano EHS studies. Small 9, 1608–1618. https://doi.org/10.1002/smll.201202115.
Soroush, A., Ma, W., Silvino, Y., Rahaman, M.S., 2015. Surface modification of thin film composite forward osmosis membrane by silver-decorated graphene-oxide nanosheets. Environ. Sci. Nano 2, 395–405. https://doi.org/10.1039/c5en00086f.
Su, Y., Yang, G., Lu, K., Petersen, E.J., Mao, L., 2017. Colloidal properties and stability of aqueous suspensions of few-layer graphene: Importance of graphene concentration. Environ. Pollut. 220, 469–477. https://doi.org/10.1016/j.envpol.2016.09.089.
Tang, J., Chen, Q., Xu, L., Zhang, S., Feng, L., Cheng, L., et al., 2013. Graphene Oxide – Silver Nanocomposite as a highly effective antibacterial agent with species-specific mechanisms. ACS Appl. Mater. Interfaces 5 (9), 3867–3874. https://doi.org/10.1021/am4005495.
US EPA Ecological Effects Test Guidelines Fish Acute Toxicity Mitigated by Humic Acid. United States Environ Prot Agency 1996;OPPTS 850.
Tortella, G.R., Rubilar, O., Dur, N., 2019. Silver nanoparticles: Toxicity in model organisms as an overview of its hazard for human health and the environment. J. Hazard Mater. 390. https://doi.org/10.1016/j.jhazmat.2019.121974.
Van Aerle, R., Lange, A., Moorhouse, A., Paszkiewicz, K., Ball, K., Johnston, B.D., de-Bastos, E., Booth, T., Tyler, C.R., Santos, E.M., 2013. Molecular mechanisms of toxicity of silver nanoparticles in zebrafish embryos. Environ. Sci. Technol. 47, 8005–8014. https://doi.org/10.1021/es401758d.
Wang, D., Saleh, N.B., Sun, W., Park, C.M., Shen, C., Aich, N., Peijnenburg, W.J.G.M., Zhang, W., Jin, Y., Su, C., 2019. Next-generation multifunctional carbon–metal nanohybrids for energy and environmental applications!next-generation multifunctional carbonmetal nanohybrids for energy and environmental applications. Environ. Sci. Technol. 53, 7265–7287. https://doi.org/10.1021/acs.est.9b01453.
van Pomeren, M., Brun, N.R., Peijnenburg, W.J.G.M., Vijver, M.G., 2017. Exploring uptake and biodistribution of polystyrene (nano)particles in zebrafish embryos at different developmental stages. Aquat. Toxicol. 190, 40–45. https://doi.org/10.1016/j.aquatox.2017.06.017.
Wang, H., Adeleye, A.S., Huang, Y., Li, F., Keller, A.A., 2015. Heteroaggregation of nanoparticles with biocolloids and geocolloids. Adv. Colloid Interface Sci. 226, 24–36. https://doi.org/10.1016/j.cis.2015.07.002.
Wang, Z., Zhang, L., Zhao, J., Xing, B., 2016. Environmental processes and toxicity of metallic nanoparticles in aquatic systems as affected by natural organic matter. Environ. Sci. Nano 3, 240–255. https://doi.org/10.1039/c5en00230c.
Wierzbicki, M., Jaworski, S., Sawosz, E., Jung, A., Gielerak, G., Jaremek, H., et al., 2019. Graphene Oxide in a Composite with Silver Nanoparticles Reduces the Fibroblast and Endothelial Cell Cytotoxicity of an Antibacterial Nanoplatform. Nanoscale Res. Lett. 14 https://doi.org/10.1186/s11671-019-3166-9.
Xu, J., Wang, Y., Hu, S., 2017. Nanocomposites of graphene and graphene oxides: Synthesis, molecular functionalization and application in electrochemical sensors and biosensors. a review. Microchim. Acta 184, 1–44. https://doi.org/10.1007/s00604-016-2007-0.
Yin, P.T., Shah, S., Chhowalla, M., Lee, K., 2015. Design, synthesis, and characterization of graphene – nanoparticle hybrid materials for bioapplications. Chem. Rev. 115, 2483–2531. https://doi.org/10.1021/cr500537t.
Zhang, J., Guo, W., Li, Q., Wang, Z., Liu, S., 2018. The effects and the potential mechanism of environmental transformation of metal nanoparticles on their toxicity in organisms. Environ. Sci. Nano 5, 2482–2499. https://doi.org/10.1039/c8en00688a.
Zhao, J., Lin, M., Wang, Z., Cao, X., Xing, B., 2020. Engineered nanomaterials in the environment: are they safe? Crit. Rev. Environ. Sci. Technol. 0, 1–36. https://doi.org/10.1080/10643389.2020.1764279.
Zhou, Y., Chen, R., He, T., Xu, K., Du, D., Zhao, N., Cheng, X., Yang, J., Shi, H., Lin, Y., 2016. Biomedical potential of ultrafine Ag / AgCl nanoparticles coated on graphene with special reference to antimicrobial performances and burn wound healing. ACS Appl. Mater. Interfaces 8, 15067–15075. https://doi.org/10.1021/acsami.6b03021.